We are IntechOpen, the world's leading publisher of Open Access books Built by scientists, for scientists

4,800
Open access books available

122,000
International authors and editors

135M
Downloads

Our authors are among the

154
Countries delivered to

TOP 1%
most cited scientists

12.2%
Contributors from top 500 universities

CLARIVATE ANALYTICS BOOK CITATION INDEX INDEXED

WEB OF SCIENCE™

Selection of our books indexed in the Book Citation Index in Web of Science™ Core Collection (BKCI)

Interested in publishing with us?
Contact book.department@intechopen.com

Numbers displayed above are based on latest data collected.
For more information visit www.intechopen.com

2

Based on Common Inverted Microscope to Measure UV-VIS Spectra of Single Oil-Gas Inclusions and Colour Analysis

Ailing Yang
Ocean University of China
China

1. Introduction

Hydrocarbon fluid inclusions occur in a variety of geological environments, most commonly within carbonate rocks from petroliferous sedimentary (Stasiuk & Snowdon,1997). Oil-gas inclusions (OGIs) belong to hydrocarbon inclusions. The sizes of OGIs are usually in the range of 5-20μm. A micro-mass (ng-fg) palaeo-oils were trapped in a single OGI. The interaction between OGIs and outside is relative weak although a long geological age elapsing. The OGI can be seen as a closed system. In this way, an intact (not cracked) OGI can be seen as a micro-oil-gas reservoir. The OGIs take rich information about the palaeo-oils. Generally, in the evolution of the oil-gas reservoir, with the deposition depth increasing, the stratum temperature increases. The organic macromolecules were decomposed into micromolecules. The oil maturity evolutes from low to high. Similarly, in the different digenetic stages, the types, colours and composites of the OGIs are also different. With the maturity of organism from low to high, the types of OGIs are mainly from liquid phase, liquid and gas phase to gas phase. The colours change from colourless, yellow, and brown to black (Liu, Y. R. *et al.*, 2003, as cited in Burruss R.C.,1991). Micro-fluorescence properties of OGIs, largely controlled by the aromatic characteristics of the hydrocarbons, are a signature of the organic chemical composition. This phenomenon was often used to distinguish OGIs from saltwater inclusions. By different fluorescence colours of OGIs, the oil and gas charge history and oil-gas maturity are qualitatively determined. And by the abundance of grains containing OGIs (GOI)(Liu, K. Y. & Eadington, 2005, as cited in Eadington, 1996), the petroleum characteristics of the corresponding strata can be qualitatively estimated. The micro-spectroscopy is very important to OGIs and mainly includes VIS and UV-VIS spectra.

1.1 The VIS spectra technique

The VIS spectra technique includes fluorescence micro photometry (FMP), fluorescence alteration of multiple macerals (FAMM) and laser scanning confocal microscope (LSCM).

1.1.1 Fluorescence micro photometry (FMP)

FMP is a technique combined microscope and photometer (see Fig.1). Generally, the exciting source is UV light (365 nm, called internal light source in this chapter) from a mercury arc

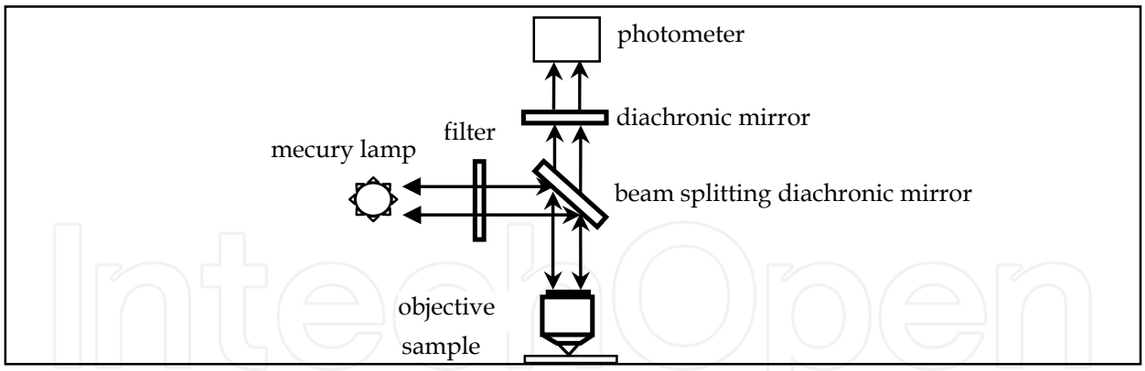

Fig. 1. A schematic diagram of a FMP. The upright microscope includes in a beam splitting diachronic mirror (with higher reflectivity to the incident light and also a higher transmittance to the fluorescence) and a diachronic mirror (absorbing the scattered light from the sample, with a higher transmission to the fluorescence).

lamp in a microscope. The UV light is focused by an objective and incidents onto a sample. The sample absorbs the exciting photons then emits fluorescence. The wavelengths of the fluorescence are longer than that of the incident light.

Some fluorescence backs (upward for the upright microscope and downward for the inverted microscope) and is collected by the same microscope objective. That light enters into the aperture of the photometer and the intensity is measured. For the inverted microscope, except for the downward fluorescence, one can measure the upward (transmitted) fluorescence because there is a big space above the sample stage to connect a photometer with the body of the microscope.

According to different study contents, one can choose different filter, beam splitting diachronic mirror, diachronic mirror and detector to realize fluorescence, transmission, reflective and absorption measurement. For example, in Fig. 1, if the photometer is an energy meter, one can measure the intensity of the fluorescence. And if the diachronic mirror has a higher absorption to the fluorescence and a higher transmission to the scattered light from the sample, the reflectivity of the sample can be measured. MPV3-microphotometer is an example. It was widely used to measure the vitrinite reflectivity of coal and source rock (Xiao *et al*., 1998, 2000).

The superiors of the above FMP are simple and low cost. But there are still some shortcomings. The first is one can only gain visible spectra (400-780 nm) for the exciting light is at 365nm. But some aromatic hydrocarbons emit UV fluorescence which can not be measured by above method. The second is the pin hole (about 0.15 mm) to limit the incident light spot often larger than the under studied OGI. Not only the under studied OGI emits fluorescence, but also other OGIs, the cements around the mineral grain trapping the OGI and even the mineral grain itself. The other OGIs may not be the same generation as the under studied OGI. What' more, the intensities of the cements are usually stronger than that of the under studied OGI. That means the fluorescence of the under studied OGI often mixes with other fluorescence. This makes the OGI looks like involving into a colourful cloud. So one can see if the size of the incident light spot is larger than that of the under studied OGI, the measured fluorescence spectrum may include the fluorescence of other OGIs, the cements around the mineral grain trapping the OGI and even the mineral grain

itself. This will lead to a decreasing reliability. So one should be cautious to judge the oil and gas charge history and oil-gas maturity by the fluorescence colours of the OGIs.

In 1997, Stasiuk *et al*. (Stasiuk & Snowdon,1997) used Zeiss MPV II to study the fluorescence of OGIs. The wavelength of the exciting light is 365 nm. A 2.5-5 μm light spot was obtained by a pin hole. The size of the light spot is less than that of the OGIs. The authors measured the micro-fluorescence spectra of artificially synthesized and natural hydrocarbon inclusions. The fluorescence spectra were related with the chemical constitutes, API degree and other geochemistry parameters of crude oils. The migration of oil and gas was revealed. The crude oils used to synthesize the artificial hydrocarbon inclusions composite a wide range of saturated hydrocarbons, aromatic hydrocarbons and NSO compounds. And also span a long geologic time (Ordovician, Devonian, Carboniferous, Jurassic and Cretaceous). For the artificial hydrocarbon inclusions, the spectra are the real spectra for single hydrocarbon inclusions. And for the natural inclusions, there are some organic compounds in the mineral grains difficult to be observed even under the microscope, so strictly speaking, the fluorescence spectra of natural inclusions are the addition of the inclusions and the mineral matrix. The results showed that most artificially synthesized hydrocarbon inclusions have main colours. A small amount have other colours. The authors gave a detailed analysis between the peak position L_{max}, Q index (Q=Intensity @ 650 nm / Intensity @ 500 nm) of the fluorescence spectra and saturated hydrocarbons, aromatic hydrocarbons, NSO compounds, nC_{18}/Ph、nC_{18}/Pr , API degree of the crude oils. The results showed the correlative factors between the peak position L_{max} and the saturated hydrocarbons, Q index and saturated hydrocarbons are all up to 0.84. Q index can be used to indicate the maturities of the crude oils.

Caja *et al*. (Caja, 2007, 2009) measured the fluorescence spectra of hydrocarbon inclusions. The results showed that Q_{580} index (580-700nm vs 400-580nm areas) is very sensitive to the total composites of the petroleum. The higher the Q_{580} index, the heavier the crude oil and the tighter relation with the API degree. For the hydrocarbon inclusions emitting yellow fluorescence, the API degree is in the range of 15-22. And for the hydrocarbon inclusions radiating blue fluorescence, the API degree is in the range of 23-45.

1.1.2 Fluorescence alteration of multiple macerals (FAMM)

In 1990s, CSITRO of Australia established FAMM. This technique combined laser with microscope. For laser has good monochromaticity and high intensity, a micrometer light spot can be easily obtained, which enhances the space resolution of the setup. By means of micro-Raman setup, assuming Ar+ laser as exciting light source (488 nm), a focal spot as less as several micrometer was obtained. The emitting intensities of source rocks at 625 nm were detected with time changing. Wilkins (Wilkins *et al*., 1992, 1995) probed the relation between vitrinite inhibiting and the fluorescence intensity changing with time. The result showed that FAMM can effectively correct inhibiting effect of vitrinite reflectivity before the stage of high maturity. Lo (Lo, *et al*., 1997) and Veld (Veld *et al*.,1997) used this technique to measure the maturity of source rock. With the help of FAMM, Xiao (Xiao *et al*., 2002) used a laser induced fluorescence microscopy (LIFM) to study the maturities of carbonate rocks with higher maturities.

FAMM and LIFM techniques are not very fitful to measure the fluorescence spectra of single OGIs. After assuming laser, one can measure the fluorescence spectra, but can not

directively observe the sample by eyes because the laser safety threshold for human eyes is less than 5 μW (Sliney D. H. ,1995). For most matters, the absorption bands are in the range of UV. But the wavelengths of Ar^+ ion laser are 488 nm and 515 nm, they don't mach well with the absorption bands of materials. So it is not very well to use Ar^+ ion laser to excite the fluorescence of single OGI. The focused laser has a higher radiation flux density at the sample surface and easily damages the sample. The changing fluorescence intensities at 625 nm with time may be relevant to the Photolysis (Sanches S., 2011) and photo polymerization of vitrinite in the coal and source rock.

1.1.3 Laser scanning confocal microscope (LSCM)

LSCM was realized in 1980s. Fig. 2 is a schematic diagram of a LSCM. The illuminating pinhole and the detector pinhole are conjugate to the focal plane of the objective. A point on the focal plane of the objective is focused at the illuminating and detecting pinholes at the same time. The other points out of the focal plane of the objective have not images at the detecting pinhole. This means confocal. A point light source illuminating and a point image are realized by an illuminating pinhole before the laser and a detecting pinhole before the detector. The light passes through the detecting pinhole will be received by a PMT or a cCCD and quickly imaged in a computer. The images have higher space resolution and good quality. By controlling the movement of the objective, LSCM can realize continues optical section by tomography similar to CT. After computer 3D imaging, a 3D profile of a micro sample can be recovered.

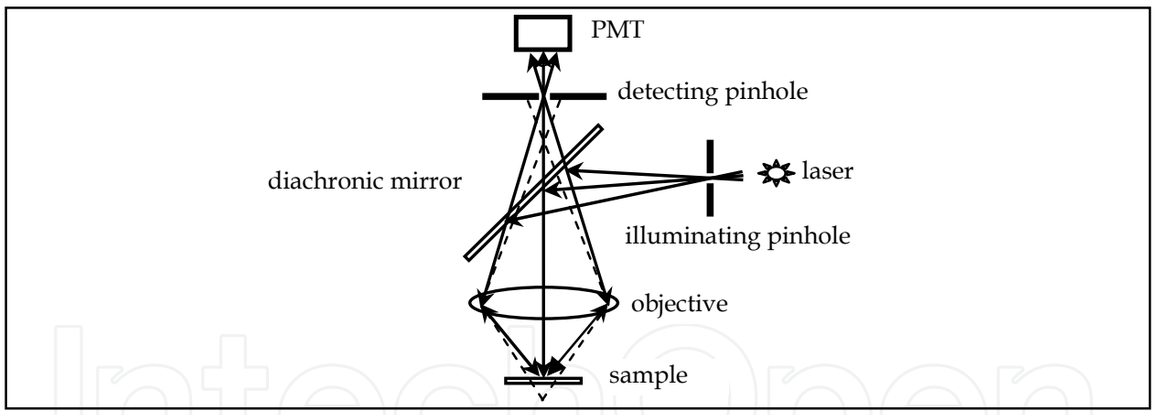

Fig. 2. The schematic diagram of a LSCM.

LSCM has been widely used in cytobiology, cytophysiology, neurophysiology and other modern medicine and biology relative to cells (Damaskinos *et al*., 1995; Kevin, 2003). It has been a forceful tool in the field of bio-science. Recently, LSCM was used to obtain precise volume ratios between liquid and gas phases in OGIs. Combining homogenous temperature, GC-MS analysis and PVTsim software, the pressure of palaeo-liquid can be obtained (Aplin *et al*., 1999; Thiéry *et al*. 2002, Liu, D. H. *et al*., 2003). Further more, the depths of the strata existing palaeo-liquids can also be obtained by the pressure. This is meaningful to study the migration of oil, gas and reservoir formation.

LSCM has special superiors as resolving the fluorescent macerals with micrometer sizes (source rock and oil shale). Stasiuk (Stasiuk, 1999) used LSCM to observe algae in oil shale.

LSCM can effectively resolve the cellular tissue in the algae. The author observed that algae have stable outermost cell wall predominance. The result assured kerogen has a selected preservation during the formation. LSCM was also used to obtain images about the space distribution of organism in mineral slides. Stasiuk (Stasiuk, 2001) measured fluorescence spectra of lipoids and chlorophyll originated from diatom. The mineral slides in the Saanich Inlet region are in rich spore oil and reproductive spore, which is relative to the periodic spore blooming in the spring. The results under the LSCM may be the preservation of spore oil at suitable depth.

Although LSCM has a higher space resolution and good image quality, till now the shortest laser wavelength of semiconductor laser is 370nm, the fluorescence of single OGI is still in the range of VIS.

1.2 The UV-VIS spectra technique for single OGIs

As above mentioned, some organic composites in OGIs emit fluorescence at UV range. So it is necessary to develop UV-VIS spectra technique.

For overcoming above drawbacks, Kihle (Kihle, 1995) established an UV-VIS micro-spectroscopy for measuring excitation-emission spectra of single OGIs. The setup includes an upright tri-ocular deep ultraviolet (DUV) microscope, a condensed lens, a collimated objective, two fiber adaptors, two fiber cables, and an UV-VIS spectrometer. The DUV microscope is very expensive comparing with the common fluorescence microscope. But for measuring the UV-VIS spectra of single OGIs, it had to be used. The spectrometer was connected with the microscope by the two fiber cables, the condensed lens, the collimated objective and the two fiber adaptors. The spectrometer supplies the exciting light in the range of 220-900 nm and record the UV-VIS spectra.

The setup could successfully measure the UV-VIS spectra of single OGIs. But there are four points to be noted. The first is for obtaining a small focal point, one has to replace the original focusing mirror of the microscope itself with a condensed mirror which was settled down on a 3D adjustable adaptor. The second is the C-mount was connected with the fiber cable not a videograph head as origin. So one can only observe the sample by ocular and can't take photos of the samples or get the sizes of the single OGIs and focusing point precisely. The third is the expensive DUV microscope, its price is 9-20 times of a common fluorescence microscope. This will greatly limit it using. The fourth is that for effective collecting fluorescence an oil immersed objective had to be used, which is trouble to clean.

The above experimental system is so expensive and one has to rebuild the microscope. Is it possible to replace the DUV microscope with a common microscope to lower cost and still detect UV-VIS fluorescence spectra of single OGIs? Such kind of micro-spectroscopy system to meet this aim was established (Yang, 2009a, 2009b, 2011). This will be given in the third section of this chapter.

2. The geology background of the samples

The sand rocks came from the core drilling samples of five oil wells (Bai 95#, Hua5#, Jian 22#, Nong 29# and Fu 4#), Jinlin Oil Filed, Songliao Basin, northeast China. Bai 95# oil well localizes in the west slope of the basin, the other are in the south to the basin. The earth

strata belong to middle to shallow, upper Cretaceous Period. The thickness of inclusion thin slide is about 150 nm.

Table 1 shows the information about the strata, depths, GOIs, average homogeneous temperatures ($\overline{T}_h s$) and salinities of the sand rocks.

There are two episodes OGIs in these samples. The first episode is in the earlier stage of quartz overgrowth, the second in the later stage of the quartz overgrowth.

Oil well	Stratum	Depth	The first episode			The second episode		
			GOI (%)	$\overline{T}_h$ (℃)	Salinity (%)	GOI (%)	$\overline{T}_h$ (℃)	Salinity (%)
Bai 95#	K_2y_{2+3}	419.3-422.1	2-3±	75.3	9.93	5-6±	113.3	4.03
	K_2y_1	426.8-436.5	3±	74.6	10.31	2±	95.4	2.98
	K_2qn_2	494.6	4±	72.3	10.95	2±	98.7	5.09
Hua 5#	K_2n_1	1449.8 1524.0	2±	\	\	0.5±	110.3	3.79
Jian 22#	K_2q_4	377.8 420.0	<1	81.0	6.77	20±	104.2	4.89
Nong 29#	K_2q_4	571.0-595.9	2±	77.0	11.34	20±	116.8	7.86
Fu 4 #	K_2q_3	419.1-426.6	2-3±	75.0	7.17	70±	135.2	4.35

Table 1. Information about the strata, depths, the measurement results of GOIs, $\overline{T}_h s$ and salinities of the sand rocks.

The GOIs, $\overline{T}_h$ s and salinities are different in the two stages. In the first episode and for all strata, except for Jian 22# oil well, the GOIs belong to middle value (Liu, K. Y. & Eadington, P., 2005, as cited in Eadington, P, 1996). In the second episode, the GOIs of Bai 95# K_2y_1, K_2qn_2 and Hua 5# K_2n_1 decrease. But for Bai 95# K_2y_{2+3} stratum, the GOI doubles. The GOIs in the second episode increase from 10 to 23 times of Jian 22#, Nong 29# and Fu 4 # oil wells, which shows there are lots of oils charging these strata in the second episode.

In the first episode, $\overline{T}_h$ s are in the range of 72.3-81.0 °C. And in the second episode, $\overline{T}_h s$ increase. The increasing amplitude is in the range of 23- 60 °C

The salinities of all strata decrease in the second episode. The $\overline{T}_h$ s and salinities show that the deposition environment has a great change in the second episode. The second episode may be in the water expanding time.

Under the fluorescence microscope, the OGIs of the first episode are liquid phase and very small. They are dense and often distribute along a line or a stripe. Their colors are often deep brown or grey brown. The fluorescence intensities are very weak. It is very difficult to measure the fluorescence of such kind of oil inclusions. The second episode OGIs are liquid or liquid-gas phases. In a mineral grain, they distribute in scattering or in group. The liquids in the OGIs are light yellow, light brown yellow, brown and grey black. Under excited at

UV, blue or green light, they often emit fluorescence. Fig.3 shows the typical OGIs in the Bai 95# oil well. Fig.3 a is a micro-photo of the first episode oil inclusions, and Fig. 3b is the second episode OGIs. Fig.3 c is the fluorescence image of Fig.3 b as excited at 365 nm (internal light source). The OGI emits light yellow fluorescence.

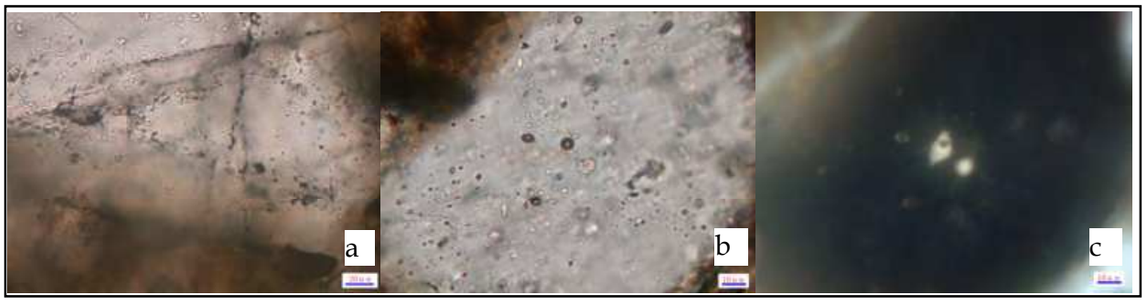

Fig. 3. The two episodes OGIs in Bai 95# oil well, in which, a is the first episode, the depth is 426.8 m; b the second episode, the depth 420.1 m; and c the fluorescence image of b under excited at 365 nm internal light source in the microscope. The scale in a is 20 μm, and in b and c 10 μm.

3. Based on common inverted microscope to measure UV-VIS spectra of single OGIs and colour analysis

3.1 The experimental setup

Fig.4 shows the schematic diagram of the experimental setup (Yang, 2009a, 2009b), which includes seven parts: (1) an inverted fluorescence microscope (IMF); (2) a reflecting microscope objective (RMO); (3) a 3D adaptor; (4) a micro lens; (5) a fiber cable; (6) a spectrometer and (7) a computer.

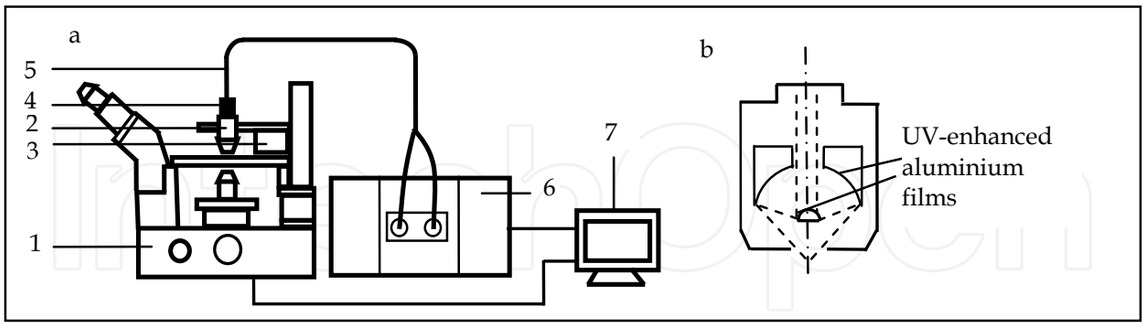

Fig. 4. Schematic diagram of the micro-spectroscopy system (a) based on common inverted microscope and the reflecting microscope objective (b). In a, 1—IMF; 2—RMO; 3—3D adaptor; 4—micro-lens; 5 —fiber cable; 6—UV-VIS spectrometer and 7—computer.

The IFM includes an internal light source (mercury arc lamp), three (violet, blue and green) standard fluorescence "cubes" bandpass filters, a dichronic mirrors and beam splitters in the optical light path. The mercury arc lamp can be used as an internal excitation source. Using bandpass filters and fluorescence "cubes", a beam with tens of nm band width can be obtained. There are five differences between this system and Kihle's setup (Kihle, 1995). (1)

A common and cheap IFM was used but not an expensive upright DUV microscope. The 3D adjustable adaptor can conveniently connected to the main body of the IFM and not need any rebuilding to the microscope. (2) It is easy to adjust the RMO and the IMF coaxial. When the switch of the IMF is on and kept the least intensity, one can adjust the 3D adjustable adaptor while observe the reflected light intensity from the RMO. When the beam intensity is maximal, the two are coaxial. (3) The RMO has many advantages over refracting objective. It is an all-reflecting construction and free from chromatic aberration. The primary spherical aberration, primary coma and primary astigmatism have been corrected. The specific mirror coating is UV-enhanced aluminium film, which has as high as 89% average reflectivity in the range of 190 nm-10 μm and is highly recommended for most UV use. Comparison with the refracting objective, the RMO has stronger focusing ability. (4) The RMO has a relative big numerical aperture (0.65), so it can be used as an excellent focusing element and also a good component to effectively collect fluorescence; (5) One can use the videohead to take photos for the samples and the focusing point in time.

In the setup, the spectrometer is FluroMax-4 (Horiba Jobin Yvon) with a 150 W xeon lamp and a single photon PMT. The RMO is made of Ealing (52X). The micro-lens and the fiber cable are from Avertise. The diameter of the fiber is 400 μm and has a 90% transmission in the range of 240-800 nm. There are seven fibers in the fiber cable. The fibres are arranged like a club. The middle one is as exciting fiber to guide the exciting light from the xenon lamp in the spectrometer to the micro-lens. The peripheral six are as emitting fibers to guide the fluorescence into the spectrometer.

The system integrates the functions of micro-area location, DUV light excitation, weak fluorescence detection and real-time taking photos together. A computer program to calculate the chromaticity coordinates of the OGIs by the spectra excited at 365 nm was also established.

3.2 The main measuring steps

For observing, taking photos and measuring the fluorescence spectra of single OGIs, there are several key steps to be noted in the experiment. To decreasing influence from environment, the experiment was done in the dark. The main steps are as following: (1) Find and localize an OGI in the middle of the visual field. Take photos when white light illuminates the OGI. (2)Take photos as exciting by UV, blue and green light of the internal light source. Be careful not make the CCD satiate. (3) Adjust the 3D adaptor and make the RMO and the objective of the IMF coaxial. When the two are coaxial, one can observe a brightest and roundest spot over the RMO. Note the power of the green light from the mercury arc lamp least and ware a goggle glasses to protect eyes. (4) Obtain a least focal spot. Connect the micro-lens with the 3D adaptor, and also the fibre cable with the micro-lens. Switch on the spectrometer, let the exciting fibre guide the 550 nm green light out of the spectrometer and get to the micro-lens and then to the RMO. The RMO focuses the exciting light into a small spot and incident on the inclusion thin slide. If the adjustment is good enough, one can see a green focal spot on the slide. According to the position of the focal spot, one should repeatedly adjust x, y, and z axes of the adjustable adaptor and decrease the size of the focal spot. For obtaining a least focal spot, one should also adjust the relative distance between the micro-lens and the RMO. Once a least focal spot appearance, this distance should be fixed and not change it in the whole experiment. (5) Take photos of single OGI excited by external light source (Xeon lamp) and record the fluorescence spectra.

The exciting and emitting slits are 10 nm and 8 nm respectively. A proper filter should be placed before the emitting window of the spectrometer. (6) Measure the micro fluorescence spectra of OGI excited by the internal light source (UV, blue and green). Note that the exciting slit of the spectrometer should be off. The emitting slit is 5 nm. (7) Measue the background fluorescence spectra when excited by external light source. The exciting wavelengths and the two slits widths are as same as step (5).

3.3 The lest focal spot of the RMO

Fig. 5 is the least focal spot of the RMO. The background is a quartz grain in an inclusion thin slide. The size of focal spot is about 12 μm. The halo light around the focal spot is the result of the diffraction. It is difficult to be eliminated for a RMO. The focal spot includes most energy.

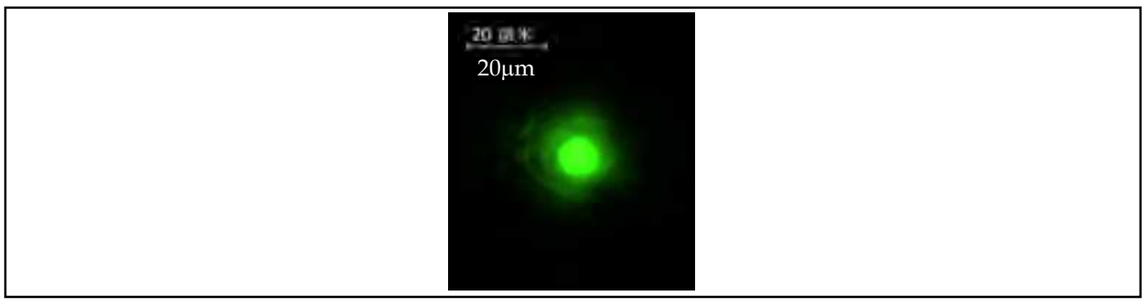

Fig. 5. The least light spot

3.4 The background fluorescence and the subtract factor

The focal spot of the RMO is not small enough. When the size of the focal spot is larger than that of the OGI, not only the OGI emits fluorescence, but also the background. The background fluorescence is complex. It may origins as following: (1) The mineral grain may include in a few even lots of micro oil inclusions (Stasiuk & Snowdon, 1997; Meng, 2009), but they can't be resolved under the IMF. (2) The surface of the mineral grain was contaminated by oils existing in the sand rock as preparing the inclusion thin slide. (3) The mineral grain may contain some thulium, which will emit fluorescence when they are excited by light. (4) The inclusion thin slide may be contaminated by organism from air or by people's hands.

Fig.6 shows the transmission micro-images of a single OGI (a, c, and e) and background (quartz grain)(b, d and f). In Fig.6 a and Fig.6 b, the exciting wavelengths are 250 nm and a violet fluorescence filter cube was used. In Fig.6 c and Fig.6 d, the exciting wavelength is 470 nm and a blue fluorescence filter cube was used. And in Fig.6 e and Fig.6 f, the 550 nm light was as exciting beam, the fluorescence filter cube was violet (The green fluorescence filter cube blocks the green light to get to the videohead, but the violet fluorescence filter cube permits the green light arrive to the videohead).

At the 550 nm light exciting, the borderline of the OGI and the focal spot are clear. This will advantage to determine the sizes of the OGI and the focal spot.

From Fig.6, one can see that the fluorescence of single OGI is the addition of the background and the OGI. For decreasing the influence of the background, a subtract factor was determined.

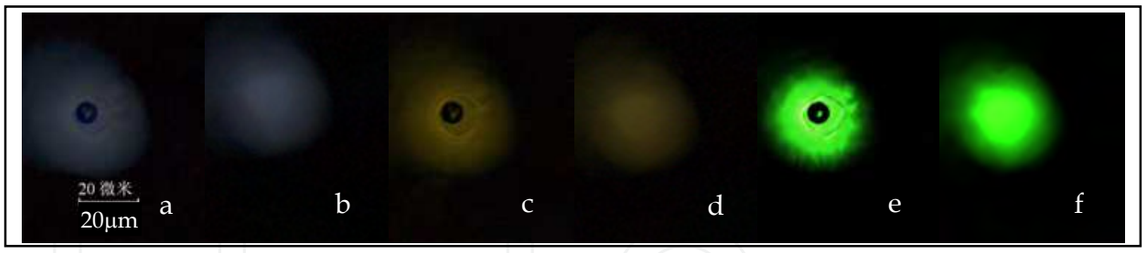

Fig. 6. Transmission micro-images of single OGI (a, c and e) and the background (b, d and f). In which, a and b, c and d, and e and f are excited at 250 nm, 470 nm and 550 nm respectively. In a, b, e, and f, the violet fluorescence filter cube was used, which has a higher transmittance to the green light. In c and d, the blue fluorescence filter cube was used.

The focal spot includes most exciting energy. The energy distribution is approximated to be homogeneous on the spot area. The OGI and the background are seen as surface light sources. Assuming the areas of the OGI and the light spot are S_1 and S_2. The two areas are easily obtained from Fig.6 e and Fig.6 f. The luminous intensities from unit surfaces of the OGI and the background are I_i and I_b. If the total fluorescence intensity of OGI and part background (S_2-S_1) is $I_1(\lambda)$, the intensity of the background is $I_2(\lambda)$. Then

$$I_1 = S_1 I_i + (S_2 - S_1) I_b \tag{1}$$

$$I_2 = S_2 I_b. \tag{2}$$

From Eq. (1) and (2), the intensity of the OGI is

$$I_i S_1 = I_1 - (1 - \frac{S_1}{S_2}) I_2 = I_1 - F I_2 \tag{3}$$

$$F = 1 - \frac{S_1}{S_2}. \tag{4}$$

Here F is the subtract factor. It can be obtained from the micro-photos of the OGI and the background. By the experiment, one can obtain I_1, I_2, S_1, and S_2. According to Eq. (3) and (4), one can further obtain the fluorescence spectra of single OGI. The following results based on above analysis.

3.5 The UV-VIS spectra of single OGIs

The first episode oil inclusions are very small and dense. The fluorescence is very weak. The background fluorescence greatly interferes the signal. The OGIs in the second episode are relative big and in scattering or in group in the mineral grains. It is possible to obtain the fluorescence spectra of single OGIs of the second episode, so these inclusions were chosen as samples.

In the experiment, we first observed dozens of OGIs in an inclusion thin slide then chose some typical OGIs to take photos and measure fluorescence spectra. The typical OGIs in an inclusion thin slide often have similar fluorescence colors. A relative clear area in the quartz

grain was chosen as background. There are 38 typical OGIs to be measured. Table 2 shows the depths, strata, sizes, phases, F factors and corresponding oil wells of 38 OGIs.

Oil well	Stratum	Depth (m)	No.	Size (μm)	Phase	F (%)
Bai 95#	K_2y_{2+3}	419.3	1	7.0, 12.3	L+G	86.0
		420.1	2	7.7, 10.1	L+G	79.0
	K_2y_1	426.8	3	4.9, 10.7	L+G	94.2
		431.0	4	8.3, 9.7	L+G	86.0
		434.5	5	7.0, 10.7	L+G	88.7
			6	7.7, 10.8	L+G	35.3
		435.0	7	12.5, 37.1	L	86.4
	K_2qn_2	494.6	8	14.1, 14.6	L+G	57.2
			9	6.5, 10.1	L	75.0
Hua 5#	K_2n_1	1449.8	10	4.5, 4.7	L+G	90.0
		1522.4	11	17.3, 53.7	L+G	42.7
		1523.0-1524.0	12*	11.1, 12.5	L+G	0.0
		1523.3	13	4.0, 4.0	L+G	96.0
Jian 22#	K_2q_4	377.8	14	16.6, 19.6	L+G	59.8
		396.6	15	9.42, 9.38	L+G	49.0
			16	15.0, 15.4	L+G	61.9
		401.9	17	9.6, 15.3	L+G	69.9
		404.7	18	5.7, 6.6	L+G	91.5
			19	21.6, 22.9	L+G	49.1
			20	10.8, 16.7	L+G	64.7
		420.0	21*	26.4, 27.1	L+G	38.3
			22	17.1, 17.1	L+G	36.6
Nong 29#	K_2q_4	571.0-572.0	23	11.0, 17.3	L+G	72.0
			24	27.2, 30.0	L+G	0.0
		573.0-574.0	25	7.4, 10.6	L+G	82.0
		595.9	26	8.7, 9.7	L+G	86.0
			27	12.7, 25.4	L+G	65.6
			28*	37.2, 37.4	L+G	0.0
			29	12.2, 25.3	L+G	50.0
Fu 4 #	K_2q_3	419.1	30	9.8, 11.7	L	81.6
			31	20.8, 24.2	L+G	39.0
		422.8	32	51.1, 71.3	L+G	0.0
			33	10.3, 15.7	L+G	62.2
			34	7.8, 13.6	L	78.0
		424.3	35	6.8, 7.0	L+G	89.2
			36*	22.6, 23.0	L+G	0.0
		425.2	37	15.9, 18.3	L+G	65.7
			38	15.5, 25.3	L+G	55.6

Table 2. The depths, strata, sizes, phases (L is liquid, and G gas), F factor and corresponding oil wells of 38 OGIs. * means the OGI is in the cement.

Fig.7-Fig.22 are the transmission, reflective micro photos and fluorescence spectra of OGIs of No.6, No.7, No.12, No.15, No.20, No.25, No.26 and No.34. No.6 and No.7 (Fig.7-Fig.10) are in Bai 95# oil well, the depths are 434.5 m and 435.0 m. No.12 (Fig.11-Fig.12) is in Hua 5# oil well, the depth is 1523-1524 m. No.15 (Fig. 13-Fig.14) and No.20（Fig.15-Fig.16）are in Jian 22# oil well, the depths are 396.6 m and 404.7 m. No. 25 (Fig.17-Fig.18) and No. 26 (Fig.19-Fig.20) are in Nong 29# oil well, the depths are 573-574 m and 595.6 m. No.34 (Fig.21-Fig.22) is in Fu 4# oil well, the depth is 422.8 m.

No.6, No.15, No.20, No.25 and No.26 are two phases (liquid and gas) inclusions. No. 7 and No.34 are single phase (liquid) oil OGIs. No.12, No.21 and No.36 are in cements. The others are all in the quartz grains.

From the micro photos, one can see when the internal light source excites the aimed OGI, not only the OGI emits fluorescence, but also other OGIs and the cements around the mineral grains. The intensities of the cements are often stronger than that of the OGIs. Even the mineral grains also emit weak fluorescence. These are the reasons why the spectra look like each other even the OGIs with different phases and colours. For example, No. 6 and No.7 OGIs are in the same oil well, the former is liquid-gas inclusion, the later is liquid phase. The spectra of the two excited by internal light source (see Fig.8 a and Fi9.10 a) are similar. Obviously, the spectra were influenced by the background. According to the spectra excited by violet light of the microscope (see Fig. 8 a and Fig.10 a, solid line), the peak positions are at 400 nm. The main aromatic hydrocarbons in the OGIs may be three or four cyclic hydrocarbons. But the other aromatic hydrocarbons in the OGIs are difficult to determine because except for the main peak, the other parts of the spectra are almost flat. The peak positions excited by the internal blue and green light are at 500-510 nm and 575 nm-600 nm respectively.

When the external light source (250 nm, 365 nm, 440 nm, 470 nm and 546 nm) excited the aimed OGI, the focal spot size is small. The cements were not illuminated, so the fluorescence spectra of the single OGIs weren't interfered by the spectra of the cements. If the OGIs are not dense in the grain, only one OGI is excited, one can obtain the spectra of single OGI after subtracting the background.

From Fig. 8 b, Fig.10 b, Fig.12 b, Fig.14 b, Fig.16 b, Fig.18 b, Fig.20 b and Fig.22 b, one can see that the spectra are in the range of UV-VIS at 250nm exciting. These results show that the experimental setup can measure the UV-VIS spectra of single OGIs. Combined the spectra excited by different external lights with different wavelengths, the characteristics of the OGIs are as following:

1. For most OGIs, when excited at 250 nm, there are three main peaks in the range of 400-470 nm, which are corresponding to three and four condensed aromatic rings, the palaeo oils are the medium Oils (Liu, K. Y., & Eadington P., 2005; Abbas *et al*., 2006). There are also two secondary peaks near to 535 nm and 610 nm, the former is the fluorescence of four or more condensed aromatic rings, the later comes from resin and asphaltene, the palaeo oils are medium and heavy Oils (Liu, K. Y., & Eadington P., 2005; Abbas *et al*., 2006). The spectra in the range of 280-400 nm belong to two or three condensed aromatic rings, the palaeo oils are light Oils (Liu, K. Y., & Eadington P., 2005; Abbas *et al*., 2006). So the OGIs of No.6, No.7, No.12, No.15, No.20, No.25 and No.34 are all filled with light, medium and heavy oils. And medium oils are the major part. The aromatic hydrocarbons in these OGIs are mainly three, four and five cyclic hydrocarbons. There

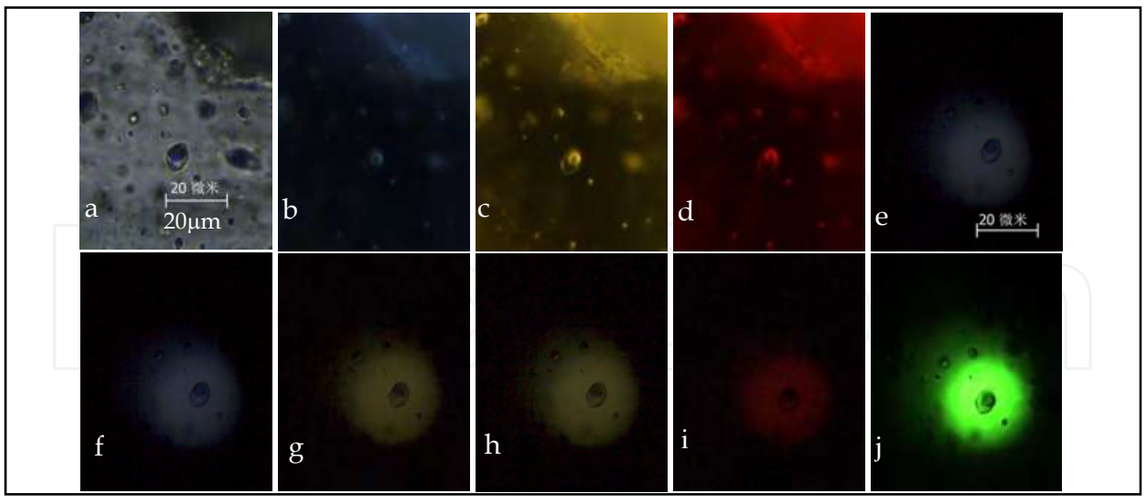

Fig. 7. The transmission (a, e, f, g, h, i and j) and reflective (b, c and d) micro-photos of No.6 OGI (Bai 95#, 434.5 m) when excited by white light (a), internal light source (c:violet; d:blue and e:green) and external light source (e:250 nm; f:365 nm; g:440 nm; h:470 nm; and i:546 nm), j is a transmission image when the 550 nm light exciting and violet fluorescence filter cube was used.

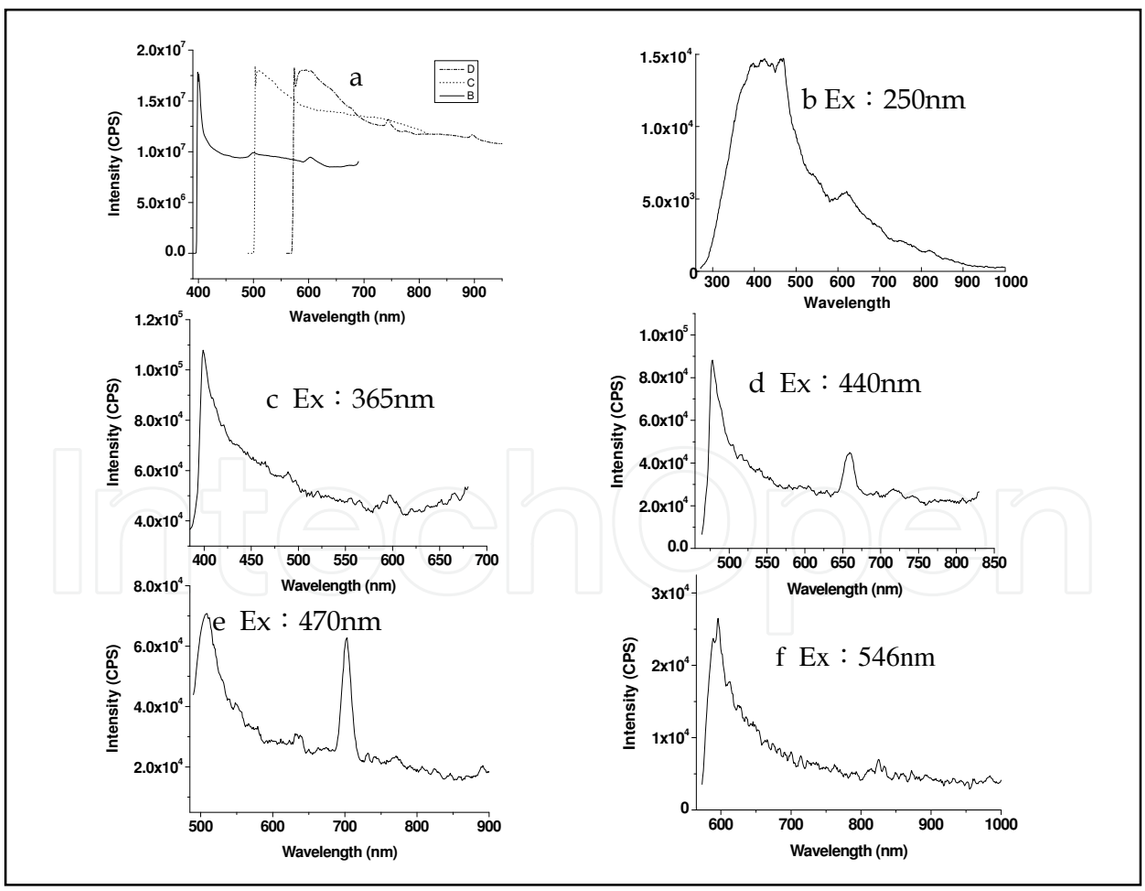

Fig. 8. The fluorescence spectra of No.6 OGI excited by internal light source (in a, solid: violet, short dot: blue, and dash dot: green) and external light source (b-f).

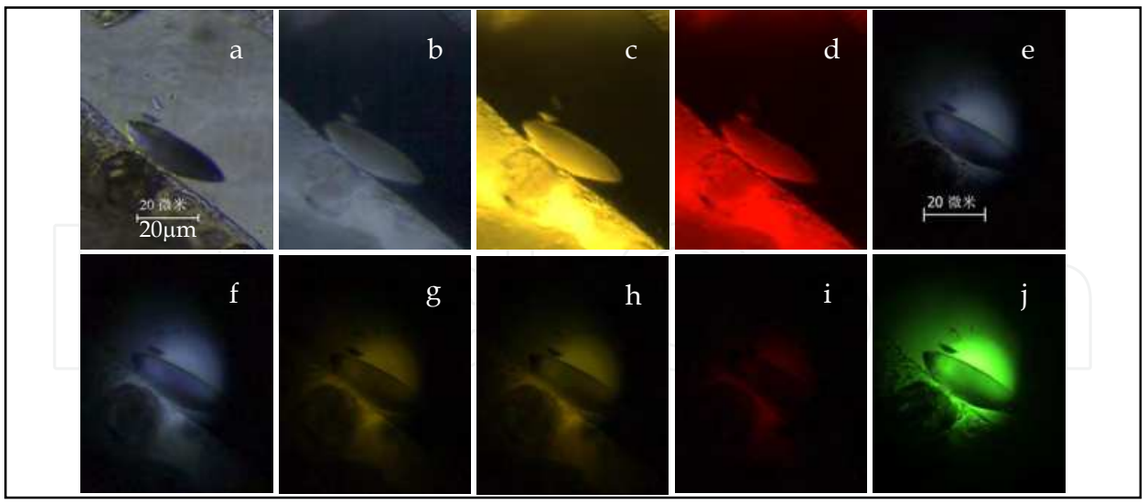

Fig. 9. The transmission (a, e, f, g, h, i and j) and reflective (b, c and d) micro-photos of No.7 OGI (Bai 95#, 435.0 m) when excited by white light (a and b), internal light source (b:violet; c:blue and d:green) and external light source (e:250 nm; f:365 nm; g:440 nm; h:470 nm and i:546 nm), j is a transmission image when the 550 nm light exciting and violet fluorescence filter cube was used.

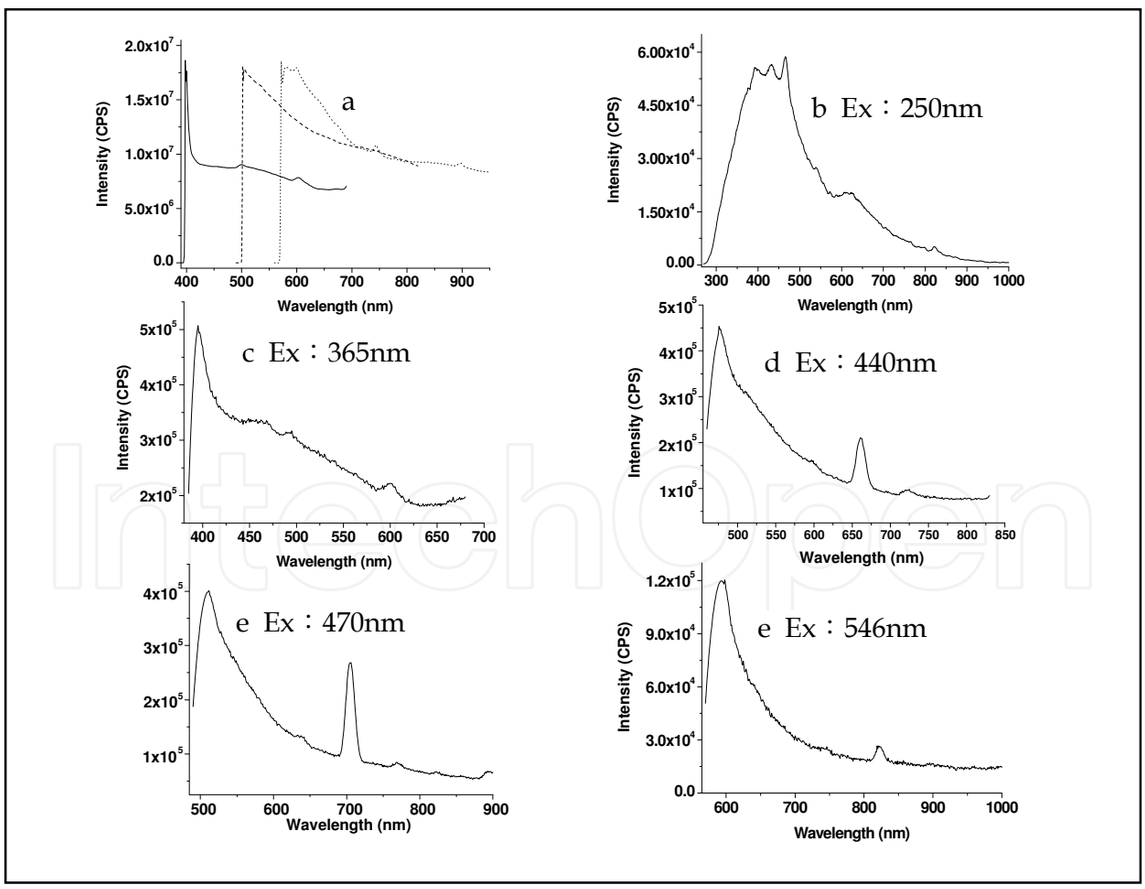

Fig. 10. The fluorescence spectra of No.7 OGI excited by internal light source (in a, solid: violet, long dot: blue, and short dot: green) and external light source (b-f).

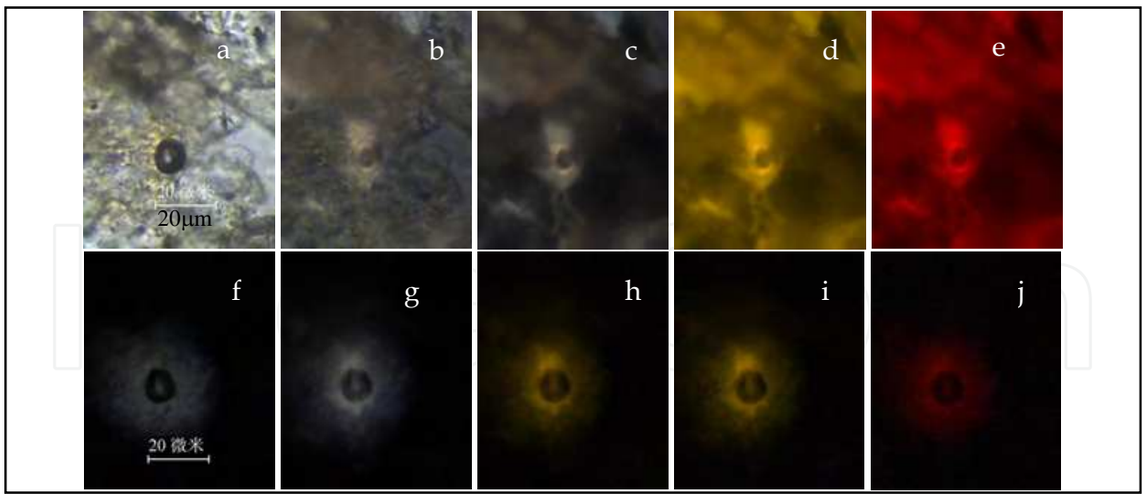

Fig. 11. The transmission (a, b, f, g, h, i and j) and reflective (b, c, d and e) micro-photos of No.12 OGI (Hua 5#, 1523.4 m) in cement when excited by white light (a and b), internal light source (b and c:violet; d:blue and e:green) and external light source (f:250 nm; g:365 nm; h:440 nm; i:470 nm and j:546 nm), b is a transmission and reflection image when white and violet light illuminating at the same time.

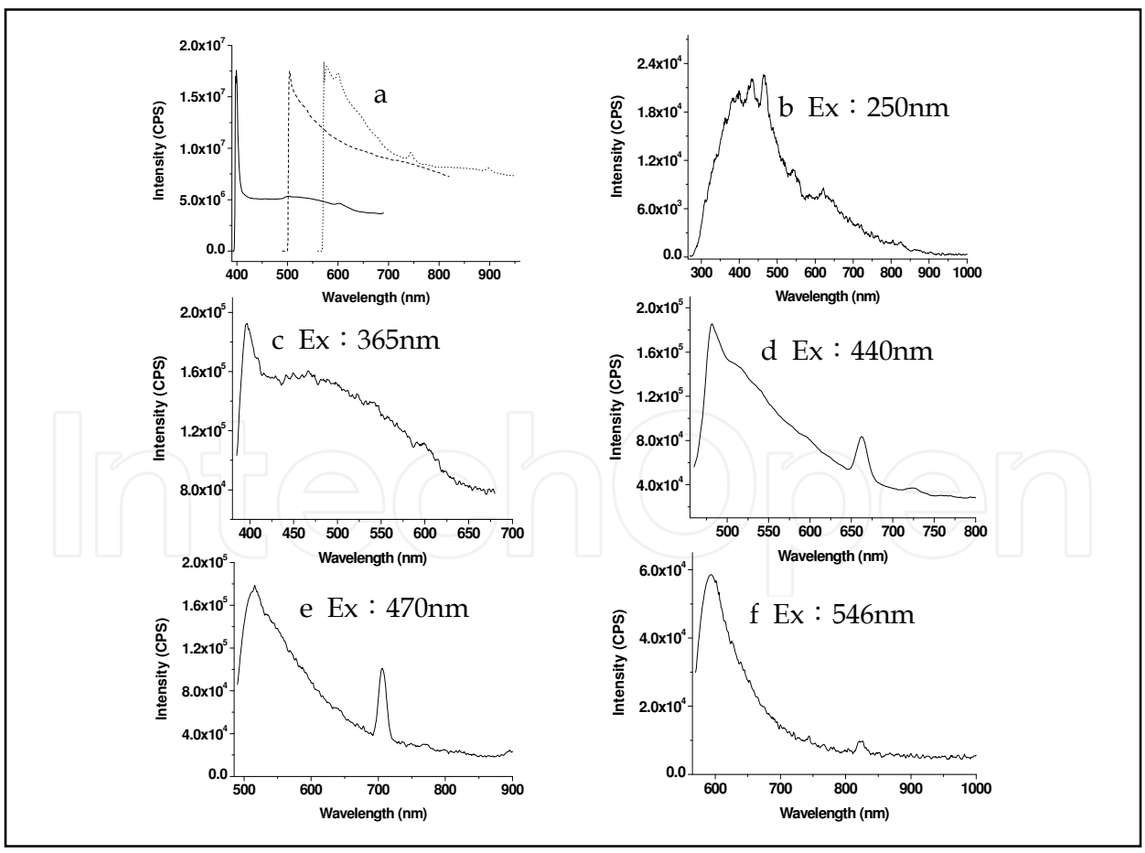

Fig. 12. The fluorescence spectra of No.12 OGI excited by internal light source (in a, solid: violet, long dot: blue, and short dot: green) and external light source (b-f).

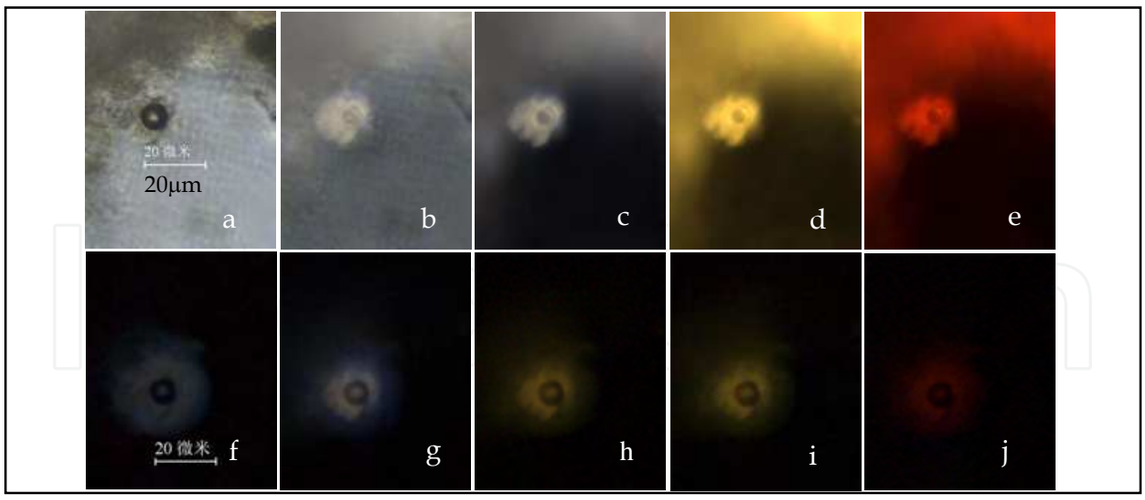

Fig. 13. The transmission (a, b, f, g, h, i and j) and reflective (b, c and d) micro-photos of No.15 OGI (Jian 22#, 396.6 m) when excited by white light (a and b), internal light source (b and c:violet, d:blue and e:green) and external light source (e:250 nm; f:365 nm; g:440 nm; h:470 nm and i:546 nm), b is a transmission and reflection image when white and violet light illuminating.

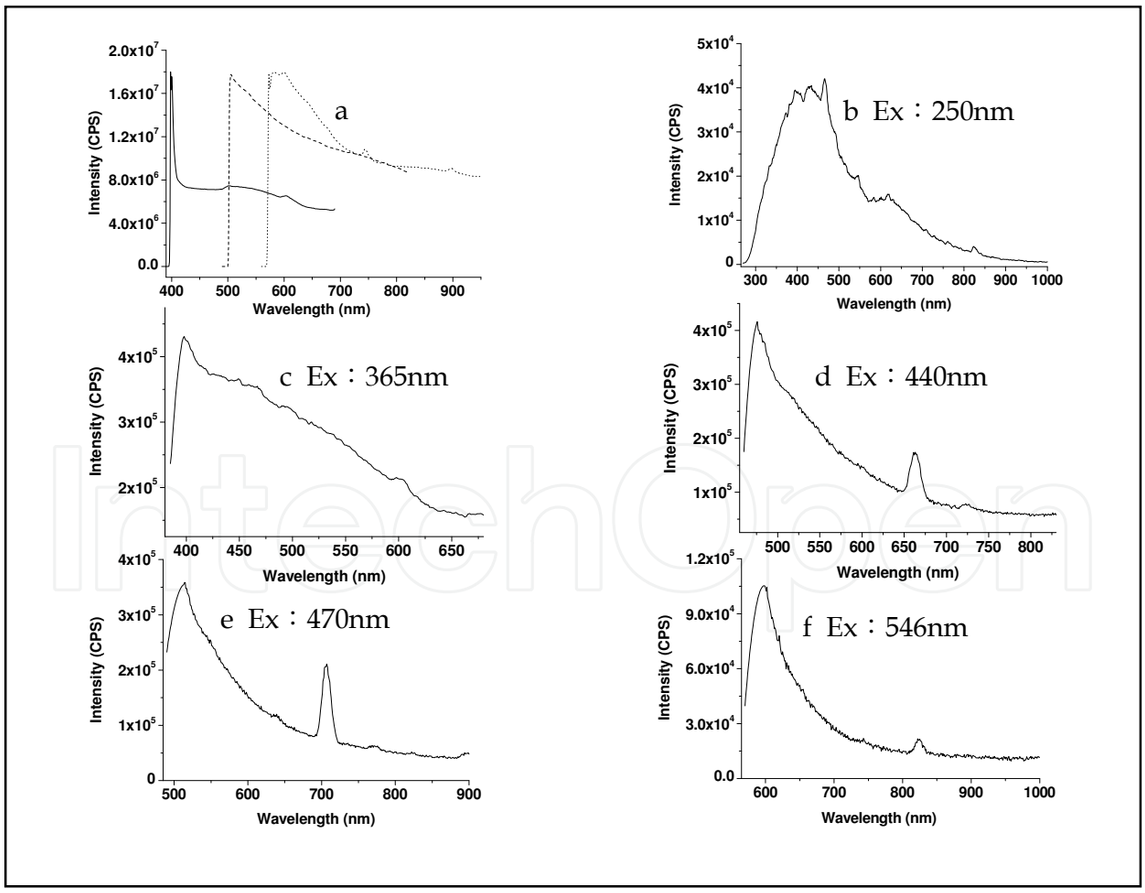

Fig. 14. The fluorescence spectra of No.15 OGI excited by internal light source (in a, solid: violet, long dot: blue, and short dot: green) and external light source (b-f).

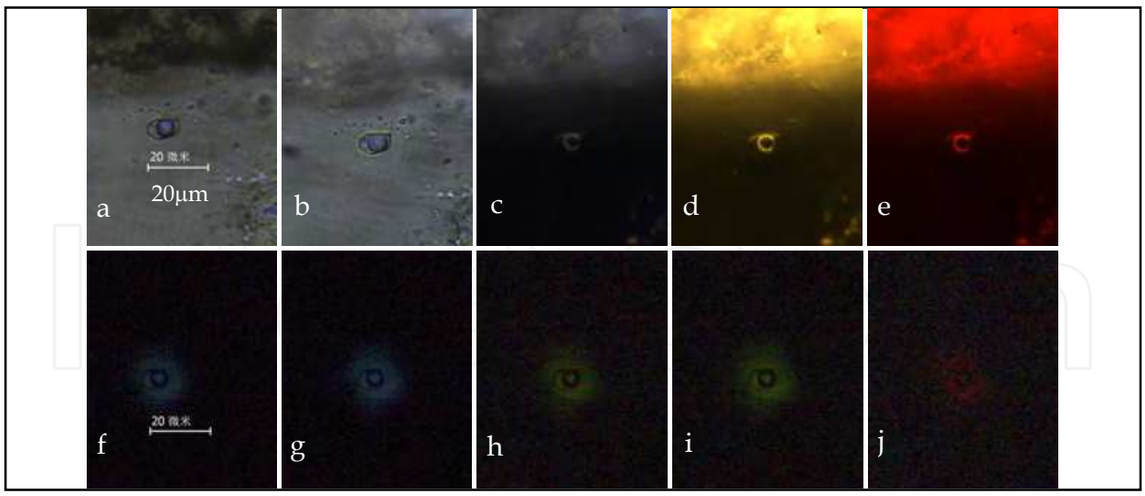

Fig. 15. The transmission (a, b, f, g, h, i and j) and reflective (b, c, d and e) micro-photos of No.20 OGI (Jian 22#, 404.7 m) when excited by white light (a and b), internal light source (b and c:violet; d:blue and e:green) and external light source (f:250 nm; g:365 nm; h:440 nm; i:470 nm and j:546 nm), b is a transmission and reflection image when white and violet light illuminating.

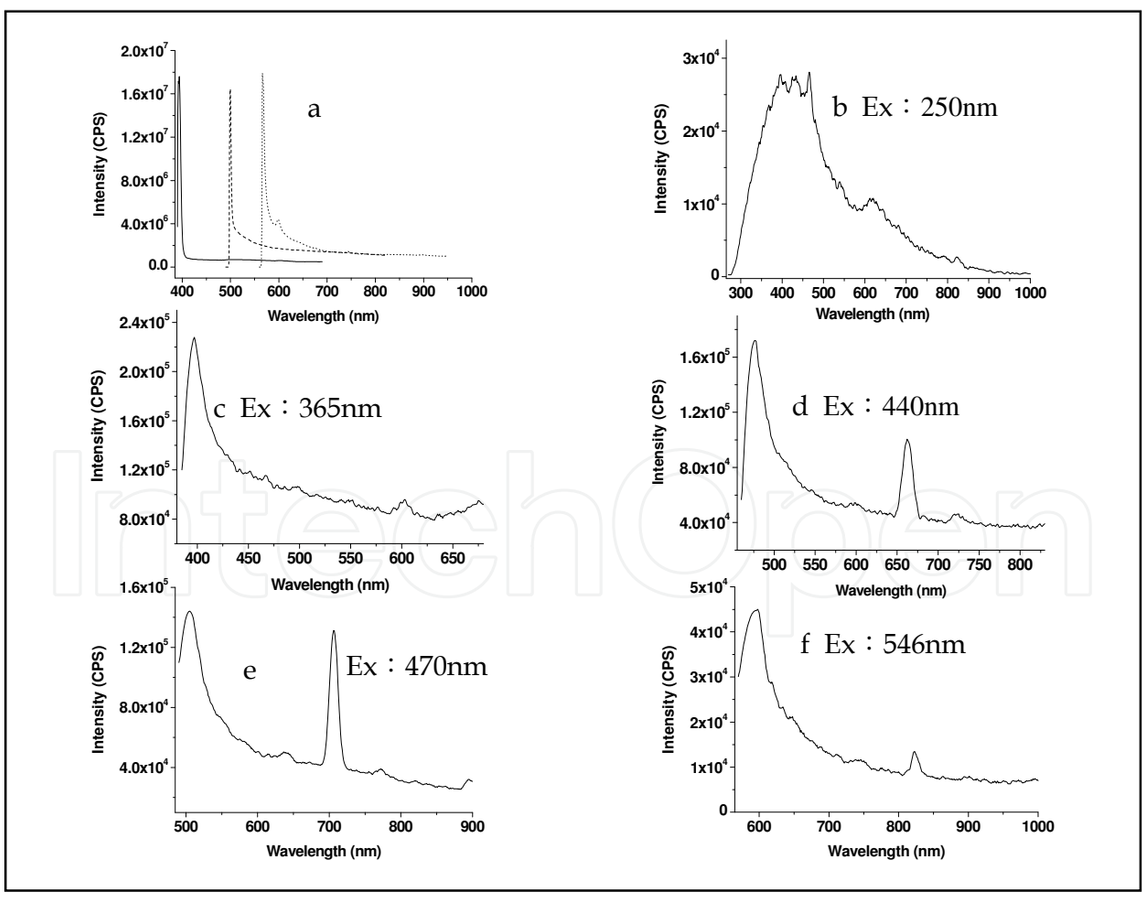

Fig. 16. The fluorescence spectra of No.20 OGI excited by internal light source (in a, solid: violet, long dot: blue, and short dot: green) and external light source (b-f).

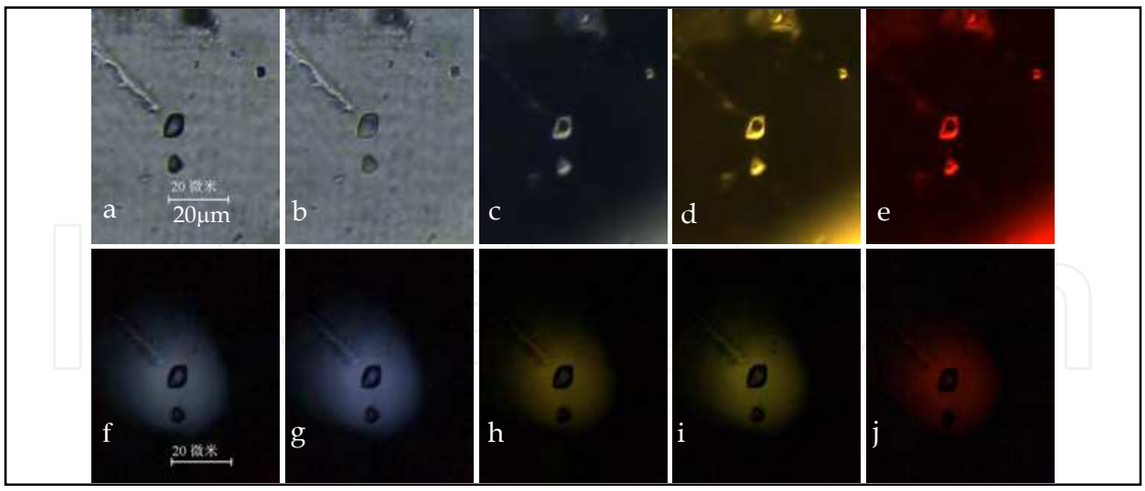

Fig. 17. The transmission (a, b, f, g, h, i and j) and reflective (b, c, d and e) micro-photos of No.25 OGI (Nong 29#, 573-574 m) when excited by white light (a and b), internal light source (b and c:violet; d:blue and e:green) and external light source (f:250 nm; g:365 nm; h:440 nm; i:470 nm and j:546 nm). b is a transmission and reflection image when white and violet light illuminating.

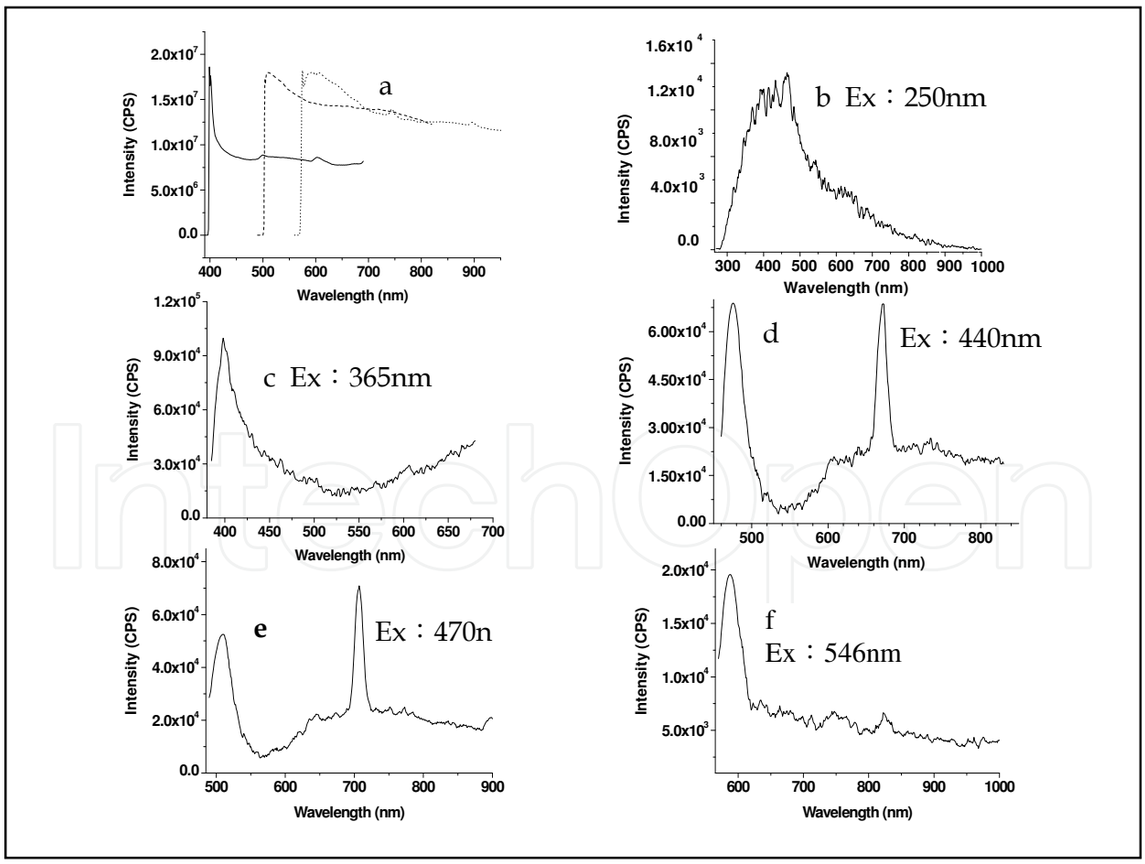

Fig. 18. The fluorescence spectra of No.25 OGI excited by internal light source (in a, solid: violet, long dot: blue, and short dot: green) and external light source (b-f).

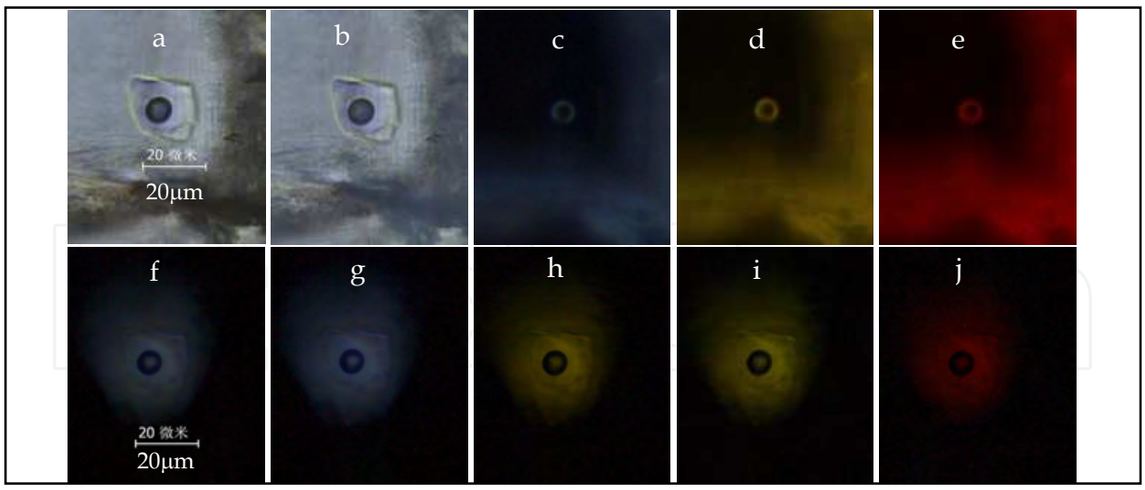

Fig. 19. The transmission (a, b, f, g, h, i and j) and reflective (b, c, d and e) micro photos of No.26 OGI (Nong 29#, 595.9 m) when excited by white light (a and b), internal light source(b and c: violet; d: blue and e: green) and external light source (f:250 nm; g:365 nm; h:440 nm; i:470 nm and j:546 nm), b is a transmission and reflection image when white and violet light illuminating.

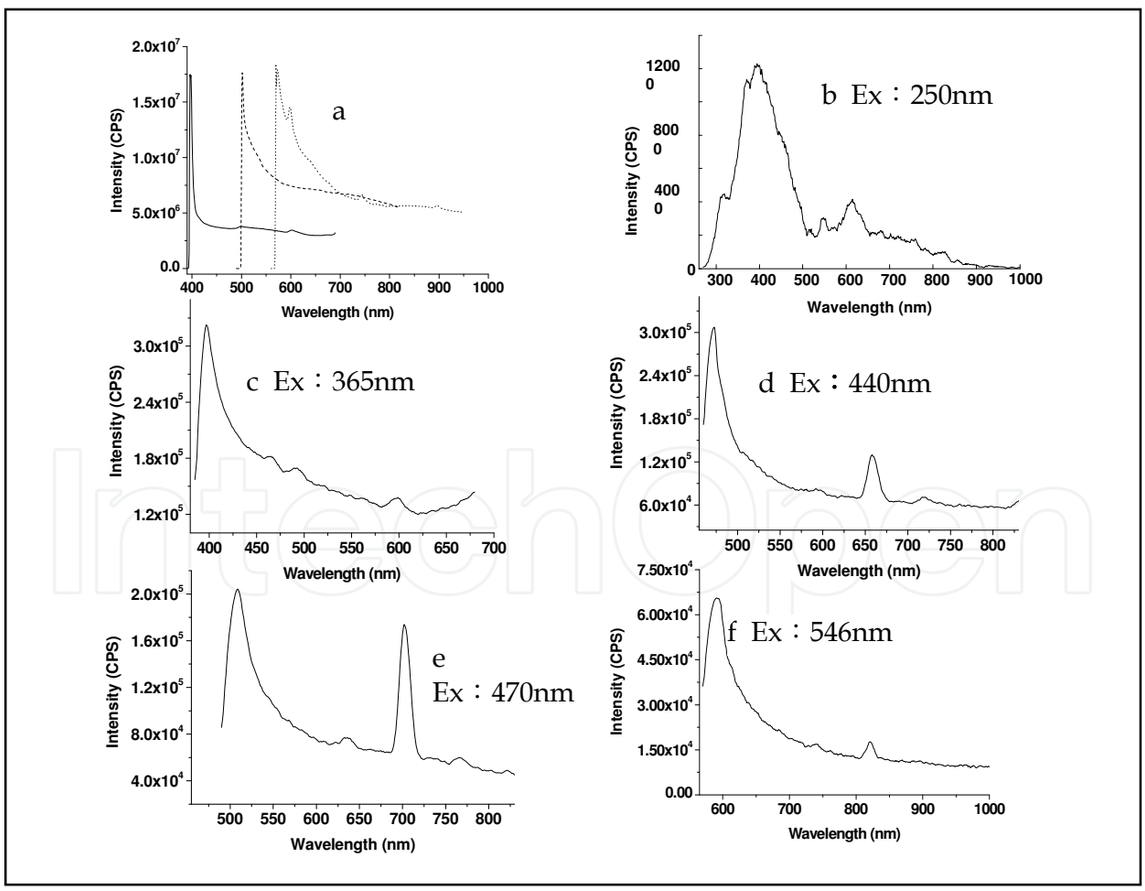

Fig. 20. The fluorescence spectra of No.25 OGI excited by internal light source (in a, solid: violet, long dot: blue, and short dot: green) and external light source (b-f).

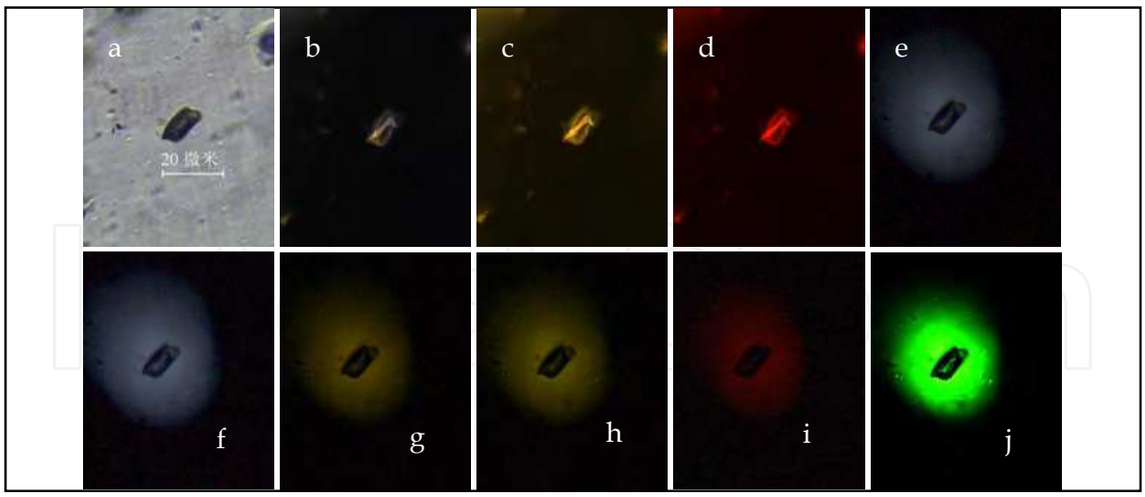

Fig. 21. The transmission (a, e, f, g, h, i and j) and reflective (b, c and d) micro-photos of No.34 OGI (Fu4# 422.8 m) when excited by white light (a), internal light source (b: iolet; c:blue and d:green) and external light source (e:250 nm; f:365 nm; g:440 nm; h:470 nm and i:546nm), j is a transmission image when the 550 nm light exciting and violet fluorescence filter cube was used.

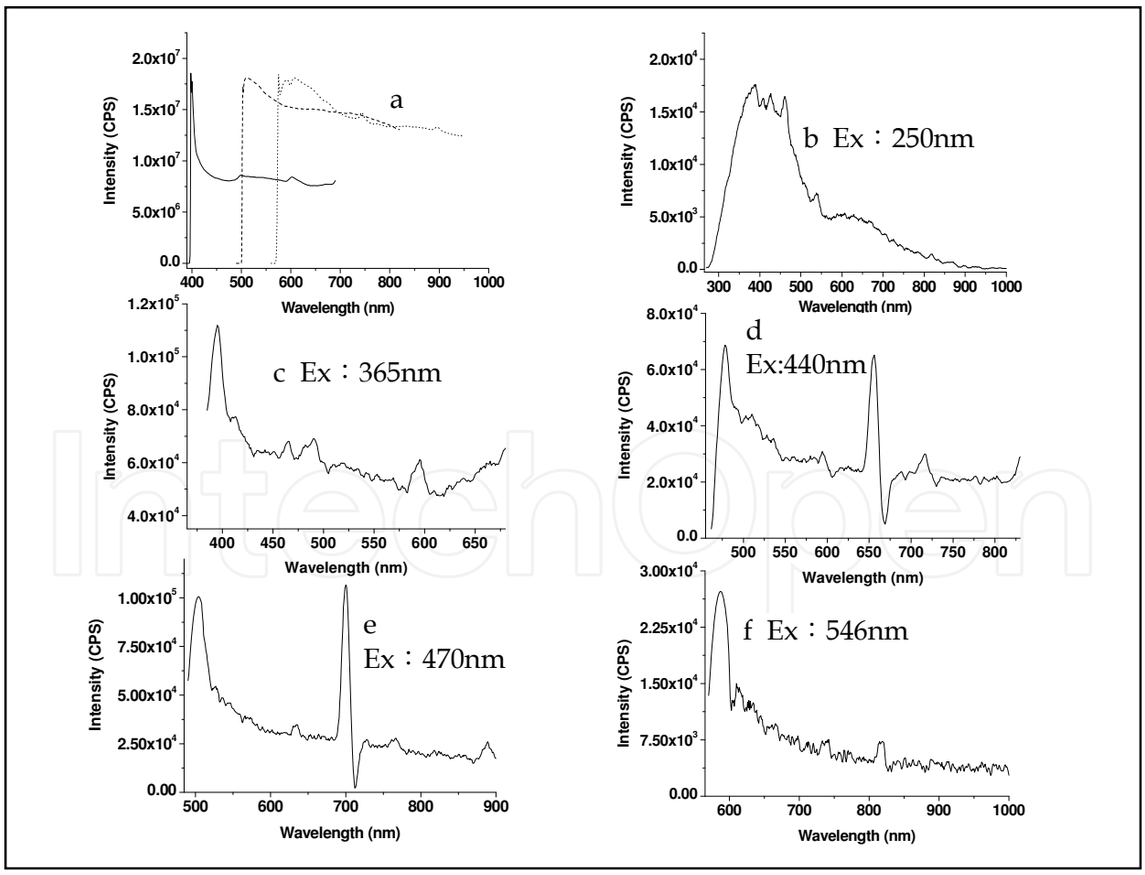

Fig. 22. The fluorescence spectra of No.34 OGI excited by internal light source (in a, solid: violet, long dot: blue, and short dot: green) and external light source (b-f).

are still some one and two cyclic aromatic hydrocarbons and heavy hydrocarbons. The spectrum (Fig.20 b) of No. 26 OGI is different from others. There is one main peak at 400 nm. The full width of half maximum (FWHM) is obviously less than the others, which shows the main hydrocarbons in this OGI are light-medium oils. The secondary peaks in 575-605 nm show there are also some heavy oils in this OGI. The aromatic hydrocarbons in No. 26 OGI are mainly three and four cyclic hydrocarbons. There are still some two cyclic aromatic hydrocarbons and heavy hydrocarbons. For all 38 testing OGIs, the spectra of 90% are similar to No.6 when exciting at 250 nm.This result shows that the palaeo-oils in the OGIs may come from two maternal sources with different maturities, one is high, another is low. So in the later time of quartz overgrowth, there may be two oil sources charging these strata at the same time.

2. In the same oil well, the FWHMs of liquid oil inclusions are wider than that of the liquid-gas OGIs at exciting 250 nm. For example, the FWHMs of No. 6 (liquid and gas) and No.7 (liquid) inclusions are 175 nm and 185 nm respectively. But in different oil wells, this result is not always right. For example, the FWHMs of No.12 and No. 15 (liquids and gas) are 189 nm and 190 nm, which are wider than that of No.7. So one should be cautious to say that the palaeo-oils in the liquid oil inclusions are more heavier than that of in the liquid and gas OGIs.
3. For all the 38 testing OGIs, when exciting at 365 nm (external light source), the spectra can be classified into two types. The first type has an obvious "bump" following the main peak. The wavelength range is in 425-650 nm. This range is relative to the medium and heavy hydrocarbons, which indicate that these inclusions including in more medium and heavy hydrocarbons (see Fig.10 c, Fig.12 c, Fig.14 c). The second type has not an obvious "bump", which shows that these OGIs (see Fig. 8 c, Fig. 16 c, Fig.18 c, Fig. 20 c and Fig.22 c) don't include in enough medium and heavy hydrocarbons as in the first type. The palaeo-oil maturities of the second type are higher than the first one.
4. When exciting at 440 nm, except for the main peak near to 478 nm, there is another peak at 657 nm for all 38 OGIs . No.25 OGI has another peak at 672 nm.
5. When exciting at 470 nm, except for the main peak near to 502 nm, there is another peak at 706 nm for all 38 OGIs.
6. The results of (4) and (5) show that a kind of characteristic matter exist in the OGIs. 440 nm and 470 nm are the effective exciting wavelengths for this kind of matter. This needs to make further analysis to determine what it is.
7. The characteristics of the spectra excited at 546 nm are not obvious. The reason is the absorption bands for the most hydrocarbons are in the range of UV and violet.

3.6 The colours of single OGIs

For simplicity and intuition, the colours of the OGIs under excited at 365 nm are often to be used to judge the maturities of palaeo-oils in the inclusions. But the judgment by eyes are subjective. The results will be influenced by psychology, physiology or environment. So it is need to calculate the chromaticity coordinates of the OGIs.

The calculation theory (Xu & Su,2004) is as following. Assume P(λ) is the power spectrum distribution of an OGI, the tristimulus values are given by equation (5),

$$X = \int_{380}^{780} P(\lambda)\overline{x}(\lambda)d\lambda$$
$$Y = \int_{380}^{780} P(\lambda)\overline{y}(\lambda)d\lambda \quad (5)$$
$$X = \int_{380}^{780} P(\lambda)\overline{z}(\lambda)d\lambda.$$

In which, $\overline{x}(\lambda)$, $\overline{y}(\lambda)$ and $\overline{z}(\lambda)$ are the tristimulus values of standard light source. One can get them by looking up the CIE 1931 system. The chromaticity coordinates of an OGI are

$$x = \frac{X}{X+Y+Z}$$
$$y = \frac{Y}{X+Y+Z} \quad (6)$$
$$z = \frac{Z}{X+Y+Z}.$$

In which, $x + y + z = 1$ (x:red; y:green and z:blue). According to above theory, a computing program based on Matlab was established to calculate the chromaticity coordinates of OGIs.

The chromaticity coordinates show that for all OGIs, the chromaticity coordinates excited by internal light source (365 nm) are larger than that of external light source (365 nm). The main reason is that not only the OGI emitting fluorescence, but also the cements and the mineral grain itself when excited by internal light source, which influenced the spectra of the under studied OGI. The chromaticity coordinates deflect to light blue white or yellow white, and relative centralize for different OGIs. When the external light source excites the OGIs, the focal spot is small. The cements don't emit fluorescence and not influence the spectra of single OGIs. The fluorescence of the mineral grain around the OGI has been subtracted as the background. Such spectra are near to the real spectra of single OGIs.

For the OGIs in the cements in Jian 22# and Fu 4# oil wells, the chromaticity coordinates of these OGIs are less than the OGIs in the mineral grains whatever external or internal light source exciting (Fig.23 c and Fig.23 e), which indicates the hydrocarbons in the cements are lighter than those in mineral grains. The formation time of the OGIs in the cements may be later than that in the mineral grains. But for OGI in cements of Nong 29# oil well, the chromaticity coordinates basic overlap with the OGIs in the mineral grains. The OGIs in the cements and in the mineral grains may be formed at the same geology age.

The chromaticity coordinates are dispersive for single OGIs under external light source excited. This result shows that it is easier to distinguish OGIs with external light source exciting. For OGIs in Bai 95# oil well, the chromaticity coordinates are in the range of light blue white and light yellow white. For OGIs in Hua 5# oil well, the chromaticity coordinates are in the range of blue green and light yellow white. For OGIs in Jian 22# oil well, the chromaticity coordinates are in the range of green blue and light yellow white. For OGIs in Nong 29# oil well, the chromaticity coordinates are in the range of light blue white and light green blue. For OGIs in Fu 4# oil well, the chromaticity coordinates are in the range of light green blue, light blue white and white. Above results indicate that in the later time of quartz overgrowth, there may be two maternal source to charge these strata, one with high maturity, another with low maturity.

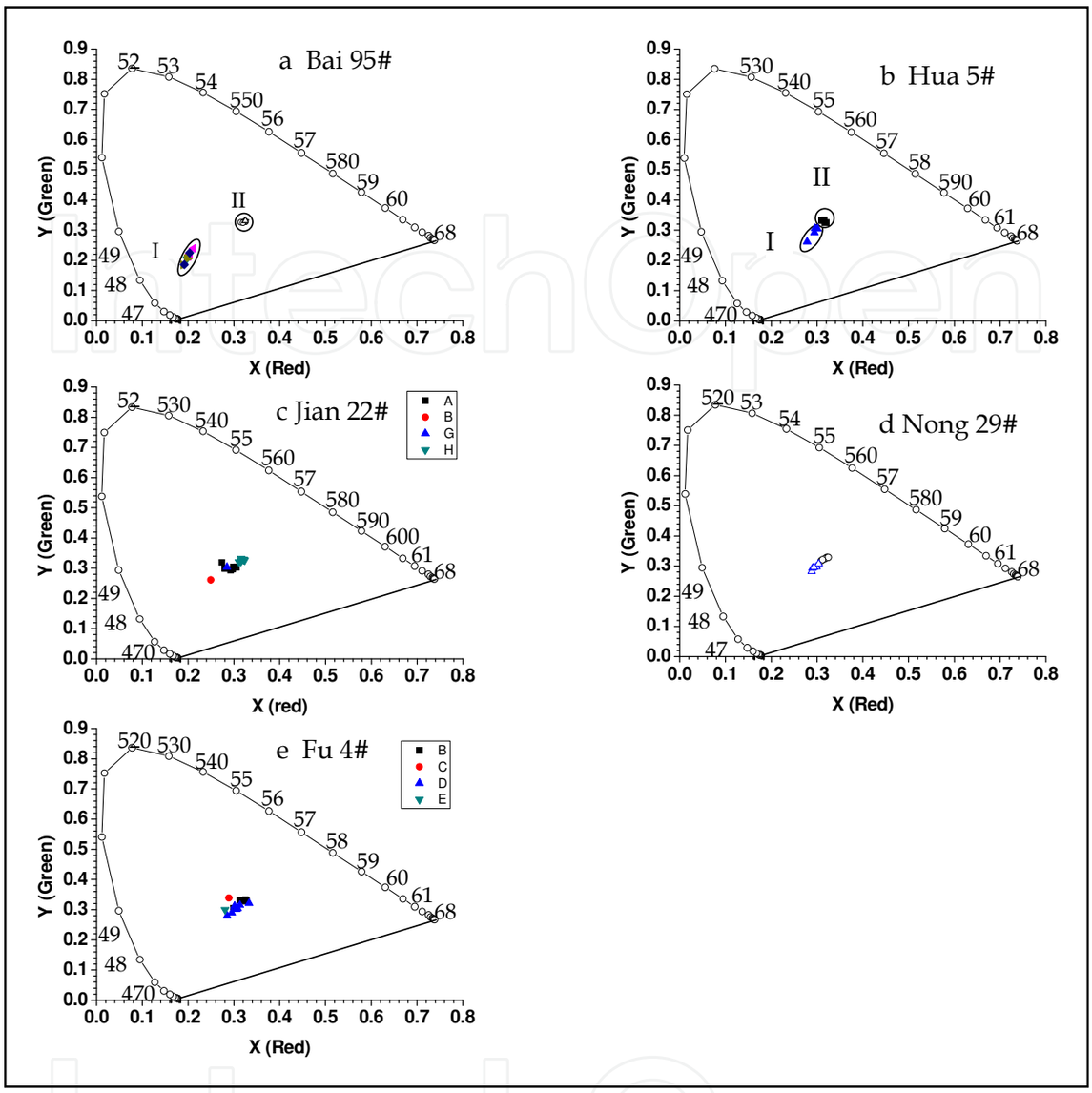

Fig. 23. The chromaticity coordinates of OGIs in the five oil wells excited by external and internal light sources, in which, a and b are Bai 95# , Hua 5# respectively, external (I) and internal (II); c—Jian 22#, external (A, B) and internal (G, H), B(G) is in the cement; d—Nong 29#, external (triangle) and internal (circle); e—Fu 4#, external (D, E) and internal (B, C), D(C) is in the cement.

4. Conclusion

The inclusion samples came from the core drilling samples of five oil wells, Jinlin Oil Filed, Songliao Basin, northeast China(upper Cretaceous Period). The microscope testing shows:

1. The experimental setup based on common inverted microscope, no need any rebuilding to the microscope and can measure the UV-VIS spectra of single OGIs. The cost was decreased greatly.

2. By the spectra excited at 250 nm, the main aromatic hydrocarbons in an OGI can be qualitative determined. Almost all OGIs contain light, medium and heavy petroleum. The main aromatic hydrocarbons are three, four and five cyclic hydrocarbons. There are also some heavy hydrocarbons and non-hydrocarbons in these OGIs. In the same oil well, the FWHMs of liquid oil inclusions are wider than that of the liquid-gas OGIs at exciting 250 nm. But in different oil wells, this result is not always right.
3. The peak positions of the spectra excited at 365 nm are in the range of 395-400 nm, the main aromatic hydrocarbons are three and four cyclic aromatics. The "bump" (425-650nm) following the main peak shows there are more medium and heavy hydrocarbons in the OGIs. The OGIs without the "bump" don't have many medium and heavy hydrocarbons. The palaeo-oil maturities of the second type are higher than the first one.
4. The special peaks near to 657 nm (440 nm exciting) and 706 nm (470 nm exciting) for all OGIs indicate there may be same special matters in these OGIs. This need further analysis combined with GC-MS and palaeo-biology.
5. The chromaticity coordinates are more dispersive for single OGIs under external light source excited than internal light source. The calculating colours excited at external light source are more objective than judging by eyes under exciting at internal light source. But one should note the different spectra may have same colour. So the spectra are important.
6. The colours, the spectra excited at 250 nm and chromaticity coordinates show that there may be two maternal sources to charge these strata in the later time of quartz overgrowth. One is high maturity, another is low maturity.

This optical system can measure UV-VIS spectra of single OGIs. For further decreasing the focal spot, one can try a 74x RMO or decrease the fiber diameter and increase the coupling efficient between the fibre and the spectrometer.

The UV-VIS spectra should be combined with GC-MS analysis to find the characteristic matter in these OGIs.

This setup is promising in measuring the fluorescence spectra of micro areas, such as bio-inclusions, micro fractures in mineral slides, special mineral grains and so on.

5. Acknowledgment

This work was supported by Chinese National Program for High Technology Research and Development (national 863 plan, granted No.2006AA09Z336) and National Natural Science Foundation of China (granted No. 41172110). The author is appreciated for Jilin Oil Field to supply sand rocks. The author greatly thanks professor Zhang, J. L., Dr. Tang., M.M., Ren, W. W. and Yang, Y. for help in the experiment.

6. References

Abbas, O., Rébufa, C., Dupuy, N., Permanyer, A., Kister, J. & Azevedo, D.A. (2006). Application of chemometric methods to synchronous UV fluorescence spectra of petroleum oils. *Fuel*, Vol. 85, No.17-18, (Dec. 2006), pp. 2653-2661, ISSN 0016-2361

Aplin, A.c., Macleod, G., Larter, S.R., Pedersen, K.S., Sorensen H. & Booth, T. (1999). Combined use of Confocal Laser Scanning Microscopyand PVT simulation for estimating the

composition and physical properties of petroleum in fluid inclusions. *Marine and Petroleum Geology*, Vol.16, No.2, (Mar., 1999), pp. 97-110, ISSN 9153-7061

Caja, M. A., Permanyer, A., Munz, I. A. & Johansen, H. (2007). Preliminary data on oil and aqueous fluid inclusions of the fracture-fill in the Corones and Armancies Fms, Eocene, SEPyrenees. *GEOGACETA*, Vol.101, (n. d. 2007), pp. 127-130, ISSN 0213683X

Caja, M. A., Permanyer, A., Kihle, J., Munz, I. A. & Johansen, H. (2009). Fluorescence quantification of oil fluid inclusions and oil shows:Implications for oil migration (Armancies Fm, South-eastern Pyrenees, Spain). *Journal of Geochemica Exploration*, Vol.101, No.1, (April, 2009), pp.16, ISSN 0375-6742

Damaskinos, S., Dixon, A. E., Ellis, K. A., & Diehl-Jones, W. L. (1995). Imaging biological specimens with the confocal scanning laser microscope/macroscope. *Micron*, Vol.26, No.6, (n.d.,1995), pp. 493-502, ISSN 0968-4328

Kevin, B., Liesbeth, P., Niek, N. S., Stefaan, C. D. S. & Joseph, D. (2003). Three-Dimensional Fluorescence Recovery after Photobleaching with the Confocal Scanning Laser Microscope. *Biophysical Journal*, Vol.85, No.4, (Oct., 2003), pp. 2240-2252, ISSN 0006-3495

Kihle, J. (1995). Adaptation of fluorescence excitation-emission micro-spectroscopy for characterization of single hydrocarbon fluid inclusions. *Organic Geochemistry*, Vol. 23, No.11-12, (Nov.-Dec. 1995), pp. 1029-1042,ISSN 0146-6380

Liu, D. H., Xiao, X. M., Mi, J. K., Li, X. Q., Shen, J. K., Song, Z. G. & Peng, P. A. (2003). Determination of trapping pressure and temperature of petroleum inclusions using PVT simulation software—a case study of Lower Ordovician carbonates from the Lunnan Low Uplift, Tarim Basin. *Marine and Petroleum Geology*, Vol.20, No.1, (Jan., 2003), pp. 29-43, ISSN 9153-7061

Liu, K. Y. & Eadington, P. (2005). Quantitative fluorescence techniques for detecting residual oils and reconstructing hydrocarbon charge history. *Organic Geochemistry*, Vol. 36, No. 7, (July, 2005), pp. 1023-1036, ISSN 0146-6380

Liu, Y. R., Lu, X. B. & He, M. C. (2003). Progress on Application of Fluid Inclusion in Petroleum Exploration. *Geology Bullet in of Mineralogy, Petrology and Geoch emistry*, Vol.22, No.3, (July, 2003), pp. 245-250, ISSN 1007-2802

Lo, H. B., Wilkins, R. W. T., Ellacott, M. V. & Buckingham, C. P. (1997). Assessing the maturity of coals and other rocks from North America using the fluorescence alteration of multiple macerals (FAMM) technique. *International Journal of Coal Geology*, Vol.33, No.1, (Jan. , 1997), pp. 61-71, ISSN 0166-5162

Meng, D. W., Wu, X.L., Fan, X.Y., Meng, X. & Zheng, J.P. & Mason, R. (2009). Submicron-sized fluid inclusions and distribution of hydrous components in jadeite, quartz and symplectite-forming minerals from UHP jadeite–quartzite in the Dabie Mountains, China: TEM and FTIR investigation. *Applied Geochemistry*, Vol.24, No.4, (April, 2009), pp. 517-526, ISSN 0883-2927

Sanches S. , Leitão C., Penetra A., Cardoso V.V. , Ferreira E., Benoliel M.J., Barreto Crespo M.T., Pereira V.J. (2011). Direct photolysis of polycyclic aromatic hydrocarbons in drinking water sources. *Journal of Hazardous Materials*, Vol. 192, (Jun. 2011), pp. 1458-1465, ISSN 0304-3894

Siegwart, R. (2001). Indirect Manipulation of a Sphere on a Flat Disk Using Force Information. *International Journal of Advanced Robotic Systems,* Vol.6, No.4, (Dec. 2009), pp. 12-16, ISSN 1729-8806

Sliney D. H. (1995). Risk assessment and laser safety. *Optics & Laser Technology*, Vol. 27, No. 5, (n. d. 1995), pp. 279-284, ISSN 0030-3092

Stasiuk, L. D. & Snowdon, L. R. (1997). Fluorescence micro-spectrometry of synthetic and natural hydrocarbon fluid inclusions:crude oil chemistry, density and application to petroleum. *Applied Geochemistry*, Vol.12, No.3, (May, 1997), pp. 229-241, ISSN 0883-2927

Stasiuk, L.D. (1999). Confocal laser scanning fluorescence microscopy of Botryococcus alginite from boghead oil shale, Boltysk, Ukraine: selective preservation of various micro-algal components. *Organic Geochemistry*, Vol.30, No.8, (Aug.,1999), pp. 1021-1026, ISSN 0146-6380

Stasiuk, L.D. & Sanei, H. (2001). Characterization of diatom-derived lipids and chlorophyll within Holocene laminites, Saanich Inlet, British Columbia, using conventional and laser scanning fluorescence microscopy. *Organic Geochemistry*, Vol.32, No. 12, (Dec., 2001), pp. 1417-1428, ISSN 0146-6380

Thiéry, R., Pironon, J., Walgenwitz, F. & Montel F. (2002). Individual characterization of petroleum fluid inclusions (composition and P–T trapping conditions) by microthermometry and confocal laser scanning microscopy: inferences from applied thermodynamics of oils. *Marine and Petroleum Geology*, Vol.19, No.7, (Aug., 2002), pp. 847-859, ISSN 9153-7061

Veld, H., Wilkins, R. W. T., Xiao, X. M. & Buckingham, C. P. (1997). A fluorescence alteration of multiple macerals (FAMM) study of Netherlands coals with "normal" and "deviating" vitrinite reflectance. *Organic Geochemistry*, Vol.26, No.3-4, (Feb., 1997), pp. 247-255, ISSN 0146-6380

Wilkins, R. W. T., Wilmshurst, J. R., Russell, N. J., Hladky, G., Ellacott, M.V. & Buckingham C. (1992). Fluorescence alteration and the suppression of vitrinite reflectance. *Organic Geochemistry,* Vol.18, No.5, (Sept., 1992), pp. 629-640, ISSN 0146-6380

Wilkins, R. W. T., Wilmshurst J.R., Hladky, G., Ellacott, M. V. & Buckingham, C. P. (1995). Should fluorescence alteration replace vitrinite reflectance as a major tool for thermal maturity determination in oil exploration? *Organic Geochemistry*, Vol.22, No.1, (Jan. , 1995), pp. 191-209, ISSN 0146-6380

Xiao, X.M., Wilkins R. W. T., Liu Z.F. & Fu, J.M. (1998). A preliminary investigation of the optical properties of asphaltene and their application to source rock evaluation. *Organic Geochemistry*, Vol.28, No. 11, (July,1998), pp. 669-676, ISSN 0146-6380

Xiao, X.M., Wilkins, R. W. T., Liu D.H. Liu, Z. F. & Fu, J. M. (2000). Investigation of thermal maturity of lower Palaeozoic hydrocarbon source rocks by means of vitrinite-like maceral reflectance — a Tarim Basin case study. *Organic Geochemistry*, Vol.31, No.10, (Oct., 2000), pp.1041-1052, ISSN 0146-6380

Xiao, X. M., Wilkins R. W. T., Liu, D. H. & Shen, J.Q. (2002). Laser-induced fluorescence microscopy—application to possible high rank and carbonate source rocks. *International Journal of Coal Geology*, Vol.5, No.2, (July, 2002), pp. 129-141, ISSN 0166-5162

Xu, X.R. & Su, Z. M. (Oct., 2004). Luminescence Theory & Luminescence Materials, Chemical Industry, ISBN: 7502554106, 9787502554101, Beijing

Yang, A.l., Zhang, J.L., Ren. W.W. & Tang. M.M. (2009a). Micro-spectroscopy system based on common inverted microscope to measure UV-VIS spectra of a micro-area. *Proceedings of SPIE 7283*, ISBN 0277-786X, Chengdu, China, Nov., 2008

Yang, A.l., Ren. W.W., Zhang, J.L., & Tang. M.M. (2009b). A micro-spectroscopy system to measure UV-VIS spectra of single hydrocarbon inclusions. *Proceedings of SPIE 7384*, ISBN 0277-786X, Beijing, China, April, 2009

Yang A.L.,Tang, M.M.,Ren. W.W.,Yang, Y. & Zhang, J.L. (2011). Investigation of the ultraviolet-visible micro-fluorescence-spectra and chromaticity of single oil inclusion. *ACTA OPTICA SINICA*, Vol.31, No.3, (Mar., 2011), pp. 0318002-1-6, ISSN 0253-2239

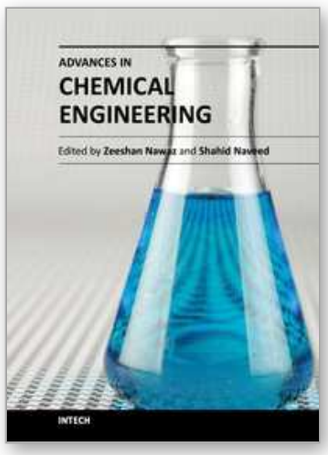

Advances in Chemical Engineering

Edited by Dr Zeeshan Nawaz

ISBN 978-953-51-0392-9
Hard cover, 584 pages
Publisher InTech
Published online 23, March, 2012
Published in print edition March, 2012

Chemical engineering applications have been a source of challenging optimization problems in terms of economics and technology. The goal of this book is to enable the reader to get instant information on fundamentals and advancements in chemical engineering. This book addresses ongoing evolutions of chemical engineering and provides overview to the sate of the art advancements. Molecular perspective is increasingly important in the refinement of kinetic and thermodynamic molding. As a result, much of the material was revised on industrial problems and their sophisticated solutions from known scientists around the world. These issues were divided in to two sections, fundamental advances and catalysis and reaction engineering. A distinct feature of this text continues to be the emphasis on molecular chemistry, reaction engineering and modeling to achieve rational and robust industrial design. Our perspective is that this background must be made available to undergraduate, graduate and professionals in an integrated manner.

InTech Europe
University Campus STeP Ri
Slavka Krautzeka 83/A
51000 Rijeka, Croatia
Phone: +385 (51) 770 447
Fax: +385 (51) 686 166
www.intechopen.com

InTech China
Unit 405, Office Block, Hotel Equatorial Shanghai
No.65, Yan An Road (West), Shanghai, 200040, China
中国上海市延安西路65号上海国际贵都大饭店办公楼405单元
Phone: +86-21-62489820
Fax: +86-21-62489821

IntechOpen